An investigation of track association algorithms for Northern Watch

Bruce McArthur
DRDC – Atlantic Research Centre

Defence Research and Development Canada

Scientific Report
DRDC-RDDC-2017-R062
May 2017

Abstract

The concept for Arctic maritime chokepoint surveillance demonstrated by Defence Research and Development Canada's (DRDC) Northern Watch project requires a process for data association—the determination that multiple data elements reported by different sensors correspond to the same detected platform—to enable the integration of information from multiple above-water and underwater sensors.

In response to documented shortfalls in the manual data association capability implemented in the Northern Watch system, this Scientific Report reviews the requirements for data association in the context of unmanned, remotely operated surveillance, and describes an investigation of one class of algorithm, based on statistical hypothesis tests, for application to the automated or semi-automated association of track data produced by the Northern Watch sensors. Two variants of the statistical hypothesis test are described—a single report test based on a pair of measurements from two sensors at a single instant in time and a multiple report test based on a sequence of measurements from each sensor. Test results are presented, using simulated data, for the association of bearings-only and positional cross-fix tracks from underwater acoustic arrays against AIS and radar tracks. It was found that association using underwater array bearings provides more consistent results when compared against similar tests involving the association of underwater array cross-fixes.

Significance to defence and security

Data association is a key enabler for the production of complete and consistent surveillance picture from multiple sensors and information sources. This work provides recommendations for the application of data association to unattended, remotely monitored, Arctic maritime chokepoint surveillance. It also provides a foundation for more extensive testing of data association using sensor data collected during the 2015 Arctic trials of DRDC's Northern Watch surveillance system.

Résumé

Le concept de surveillance des points de passage maritime obligé dans l'Arctique fournit la preuve que le projet de surveillance du Nord de Recherche et développement pour la défense Canada (RDDC) requiert un procédé d'association de données par lequel on peut établir que de multiples éléments des données recueillies par différents capteurs correspondent à une même plateforme détectée, et ce, afin de permettre l'intégration de l'information provenant de multiples capteurs en surface et sous l'eau.

En réponse aux lacunes relevées dans la capacité manuelle d'association de données mise en œuvre dans le système de surveillance du Nord, le présent rapport scientifique aborde les exigences à cet égard dans le cadre d'une télésurveillance sans opérateur et décrit l'étude d'une catégorie d'algorithmes à partir de tests d'hypothèses statistiques en vue de l'appliquer à l'association automatisée ou semi-automatisée de données de poursuite générées par les capteurs du système. Deux variantes des tests d'hypothèses statistiques sont décrites ici, soit un premier compte rendu de test unique, fondé sur les mesures provenant de deux capteurs à un instant donné, et un second compte rendu de tests multiples, fondé sur une séquence de mesures prises par chacun des capteurs. On utilise des données simulées pour comparer les résultats de tests sur l'association de pistes en mode gisement seul connu et de points par relèvements de la position à partir des réseaux acoustiques sous-marins aux pistes recueillies par sonar actif d'identification et par radar. On a découvert que l'association par mode gisement des réseaux sous-marins permettait d'obtenir des résultats plus cohérents en comparaison de ceux des points par relèvements des réseaux sous-marins.

Importance pour la défense et la sécurité

L'association de données constitue un outil clé pour produire une image de surveillance intégrale et cohérente à partir de capteurs et de sources d'information multiples. Le présent rapport comporte des recommandations en vue d'appliquer l'association de données de télésurveillance sans opérateur à la surveillance des points de passage maritime obligé dans l'Arctique. Il jette également les bases de tests d'association plus approfondis grâce aux données recueillies par des capteurs lors des essais du système de surveillance du Nord de RDDC réalisés dans l'Arctique en 2015.

Table of contents

List of figures

List of tables

1 Introduction

Northern Watch is a DRDC project that demonstrated a concept for unmanned, persistent local-area surveillance of a maritime chokepoint on Canada's Northwest Passage. The Northern Watch system included an unmanned, Arctic Surveillance Demonstration System (ASDS), located at Gascoyne Inlet, Devon Island, Nunavut, which was remotely operated from a periodically manned DRDC Southern Control Centre (DSCC), located at DRDC's Atlantic Research Centre, in Dartmouth, Nova Scotia. The ASDS included bottom-mounted underwater acoustic arrays, Automatic Identification System (AIS), Automatic Dependent Surveillance – Broadcast (ADS-B), and navigation radar, for conducting surveillance of the maritime sub-surface and surface domain, and to a secondary extent the air domain. A meteorological system was also included to provide environmental awareness at the surveillance site. The concept for the Northern Watch surveillance system is illustrated in Figure 1 and is described in detail in [1][2].

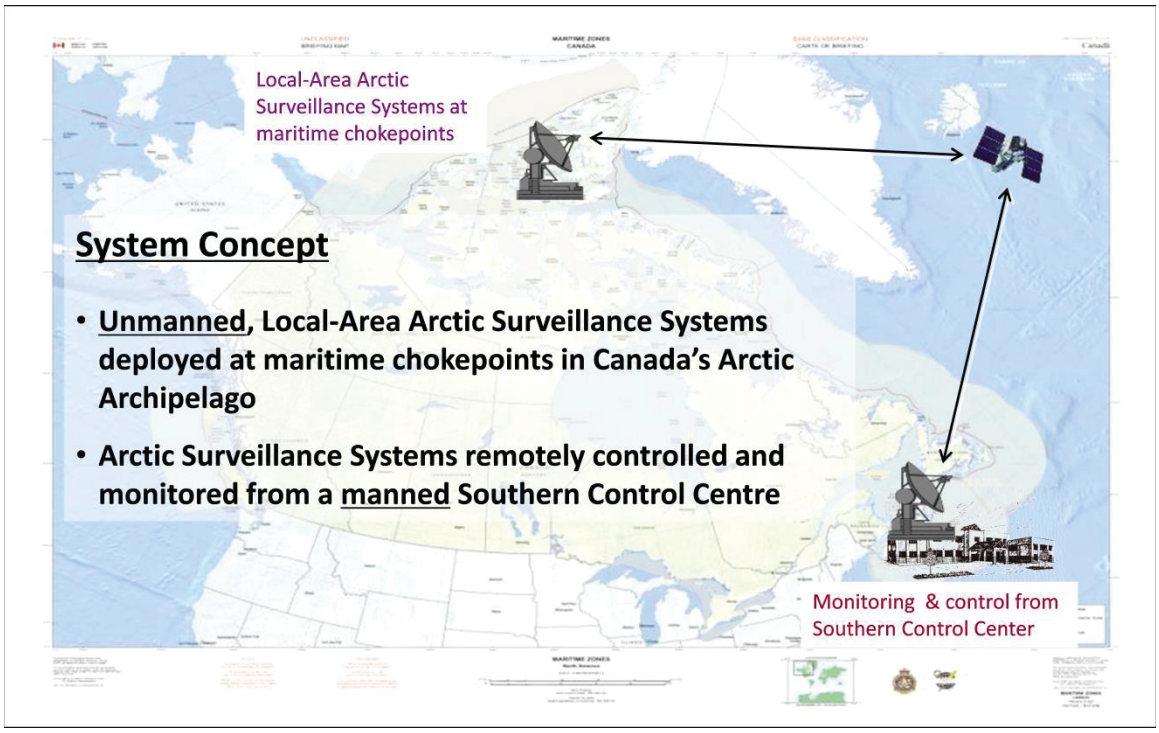

Figure 1: *Northern Watch system concept for unmanned, remotely monitored and controlled, local-area Arctic surveillance (from [3]).*

One important aspect of the Northern Watch surveillance concept is that surveillance information products contain the integrated information from multiple sensors. The benefits of data integration are well known and include [1]: "a higher probability of detecting, tracking, and classifying platforms transiting the surveillance coverage area; a more complete description of platform characteristics and activities; a lower probability of false alarm or miss-classification; and, a higher degree of confidence in the resulting surveillance products based on the use of corroborating information from multiple sources". In short, by applying a process of data integration it should be possible to increase the quality of the surveillance information products output by the Northern Watch system.

In order to integrate the data from multiple sensors, it is first necessary to determine that different data elements all correspond to the same detected platform. This process is termed data association. Data association may be implemented as a manual process performed by an operator, as a semi-automatic process, using operator decision aids, or as a completely automated process. The Northern Watch surveillance system implements a basic set of data association tools that allow an operator to manually designate sensor tracks as originating from the same source. In experimental trials of the system, conducted in August–September 2015, the manual association process was observed to be very labour-intensive and was judged to be feasible for use with only a small number of sensor tracks. Consequently, the requirement for a semi-automated or automated data association capability has been recognized as an area for future improvement of a Northern Watch system capability [3].

This Scientific Report documents an investigation of the application of statistical hypothesis tests for the automated or semi-automated association of track data produced by the Northern Watch sensors. Statistical hypothesis tests are one of several classical approaches to data association and thus represent a good starting point for the evaluation of potential algorithms. Emphasis has been placed on the association of data produced by an underwater sensor system (UWSS) with data produced by above-water sensors, such as AIS and radar. This emphasis reflects the added complexity of data produced by underwater acoustic arrays.

This investigation includes test results using simulated data for the surveillance of surface vessels using AIS, radar and UWSS sensors. The results of more extensive testing, using real sensor data collected during summer 2015 Arctic trials of the Northern Watch surveillance system, are to be provided in a separate report [4].

1.1 Organization

Section 2 begins with a background discussion on data association requirements for unattended, remotely monitored Arctic surveillance. This is followed by an overview of data association techniques and a more specific discussion of the statistical hypothesis test approach to data association.

The hypothesis test approach to data association is applied to the Northern Watch sensors in Section 3. This includes the development of simple models for each sensor and two variants of the hypothesis test—a single report test based on pairs of measurements from two sensors, obtained at a single instant in time, and a multiple report test based on a sequence of measurements from each sensor.

Section 4 presents the results of association tests between radar and AIS tracks and between UWSS and AIS tracks, using simulated data from surface surveillance scenarios. The use of UWSS bearings for association is compared against the use of UWSS cross-fixes (generated from UWSS bearings from the two underwater arrays). As well, the single report and the multiple report tests are compared using a more demanding multi-vessel scenario. Test results are evaluated on the consistency of the percentage of rejected true associations relative to the level of significance of the hypothesis test.

Finally, Section 5 provides summary conclusions as well as remarks regarding the potential utility of the hypothesis test approach for data association in support of unattended, remotely monitored Arctic surveillance.

2 Background

2.1 Data association requirements for unattended, remote monitored Arctic surveillance

According to the Northern Watch system concept [1][2], surveillance information from each detected platform is compiled from the integration of information from multiple sensors and self-reporting systems that include AIS, ADS-B, navigation radar and underwater acoustic arrays. An electro-optic/infrared camera system and a radar intercept system were part of the original system concept for Northern Watch, but were not included in the implemented system. The sensor data types transmitted from the ASDS, located at Gascoyne Inlet, to the DSCC, at DRDC Atlantic, are summarized in Table 1.

Table 1: *Data types transmitted from the Northern Watch sensors (adapted from [2]).*

Sensor	Data Type	Description
AIS	Position Report	Message types 1,3 and 18. Includes: position and velocity; ship MMSI number
	Ship Static Data Report	Message types 5 and 24. Includes: MMSI and International Maritime Organization (IMO) numbers; call sign; ship name, type, & cargo; dimensions; draught; destination & time of arrival
ADS-B	Extended Squitter Report	Includes position and velocity data; aircraft (ICAO) address, call sign, country
Radar	Track Report	Position and velocity estimates
UWSS	Bearing Report	Narrowband or broadband bearing measurements
	Cross-fix Report	Position and velocity estimates based on array cross-fixes
	Acoustic Image	Acoustic spectrogram

The production of surveillance information by the Northern Watch system can be considered from the perspective of picture compilation; with the system being used to compile a local-area Common Operating Picture (COP) of the system's surveillance coverage area. The surveillance information produced for each platform detected within the coverage area is maintained as a single consolidated track, termed a system track. Information held by a system track may include [1]:

- current and historical estimates of the position and velocity of the detected platform while it is within the surveillance coverage area. Position and velocity may be restricted to estimates of bearing and bearing rate, depending on the reporting sensor;
- classification of the detected platform, to the highest degree of precision possible, given the collected sensor data;
- the sensors or self-reporting systems reporting on the platform; and
- links to supporting data from individual sensors and self-reporting system.

One of the measures of a complete and consistent COP is the existence of a one-to-one mapping between system tracks in the COP and real-world objects detected within the surveillance coverage area. In the case of an object detected simultaneously by multiple sensors, only a single system track should be created; in other words, duplicate system tracks corresponding to the same real-world object are not desirable. Ideally, objects will be tracked continuously (using a single system track) over the time period they are within the surveillance coverage area. Maintaining a single system track for each detected object requires a decision process, termed data association, to assess whether tracks originate from the same detected object. Tracks deemed to originate from the same object are then said to be 'associated.' It is common that either the information contained in the associated tracks is combined to form a composite system track or that one of the associated tracks is selected to represent the system track, and the remaining associated tracks are supressed from the COP. Data association may be categorized according to whether one is comparing tracks from different sensors (termed intersensor association), multiple tracks produced by the same sensor (intrasensor association) or multiple tracks that are separated in time (temporal association). Data association may be performed as a manual function by an operator, automatically by the system, or semi-automatically, with the system providing an association recommendation to an operator.

The Northern Watch system is required to support the association of tracks that originate from sub-surface, surface or air objects and are generated by one or more sensors. Based on experimentation using the Northern Watch sensor suite [3][5] surface vessels can be detected by AIS, radar and UWSS, whereas the most common aircraft—high-altitude, trans-Arctic, commercial flights—are likely to be detected only by ADS-B. Local air traffic may potentially be detected by radar and UWSS, as well as by ADS-B. The UWSS provides a unique capability for detecting sub-surface platforms. It is noted that AIS and ADS-B, as self-reporting systems, do not perform traditional detection and tracking functions; rather, they receive reports of position and identity broadcast by equipped vessels and aircraft.

Based on observations of maritime traffic made in recent years, the amount of vessel traffic transiting through the surveillance coverage area of the Northern Watch system can be assumed to be at a low level. For example, the dataset collected at Gascoyne Inlet, during a 22 day period from 31 July to 21 August 2012 [5] contained a total of 15 events involving 9 different vessels.[1] No vessels were detected on 14 of the 22 days; on four days only one vessel was detected; on two days two vessels were detected; and on two days three vessels were detected. In only three instances were two vessels detected concurrently in the surveillance area; otherwise, only a single vessel was detected at a given time.

It is expected there will be a substantial variation in the numbers and characteristics of the tracks generated by different Northern Watch sensors. These, in turn, will impact on the requirements for the association of data originating from specific platform types and collected from multiple sensors. Under normal conditions, it is expected that exactly one track per platform will be broadcast by AIS and ADS-B, as both are self-reporting systems and individual AIS and ADS-B reports are labelled with the unique identifier of the broadcasting platform (either the MMSI for AIS or the ICAO number for ADS-B). Thus, even if AIS or ADS-B reports are received intermittently, we assume there is no ambiguity as to the origin of the information.

[1] DRDC's trial ship, CFAV QUEST, which was present in the surveillance area over the entire period of the trial, is not included in these numbers.

The characteristics of AIS and ABS-B tracks can be contrasted with tracks produced by the radar and UWSS systems. Radar and UWSS are sensors, as opposed to self-reporting systems, and do not share the advantage of uniquely labelling reports with the identity of the detected source. Under ideal operating conditions, the radar will also report a single track for a given detected platform. However, in non-optimal conditions, such as when detection by radar is weak or intermittent, platforms may be reported as a sequence of short tracks, separated by gaps where there have been no detections, and with individual tracks labelled with different radar-assigned track numbers. Such a situation will require a data association process to determine whether the multiple short tracks originate from the same detected platform. Tracks generated by UWSS are the most complex of any of the Northern Watch sensors for reasons that include [3][6]: the potential of generating large numbers of tracks for each detected object; bearings-only versus active sensing; conical beam patterns, that can result in a left/right ambiguity and a vertical component to bearing measurements; and three-dimensional signal propagation in the underwater acoustic environment.

The concept for the Northern Watch system assumes support for multiple modes of operator interaction together with varying levels of automation. The ASDS will be unmanned and remotely operated from the DSCC, under a combination of system and operator control. The DSCC will be manned periodically, with an operator attending to the system based either on alerts to events of interest or on a regular watch schedule. Levels of automation may vary, with manual operation being characteristic of a low level of automation, operator aids being characteristic of a medium level of automation, and automated system operation, with the operator performing a monitoring role, being characteristic of a high level of automation. Each of these modes of operation and levels of automation will impact system requirements related to data association.

Manual data association requires operator tools both to support the operator in making an association decision and to carry out the follow-on integration of information from the associated tracks. The current implementation of the Northern Watch system provides a basic set of operator tools for comparing the histories of multiple tracks [7]. If tracks originate from the same platform, then their histories when observed over a period of time should be in close agreement. For example, Figure 2 depicts the display of track histories for radar and AIS tracks originating from the HMCS SHAWINIGAN, as recorded during the final demonstration of Northern Watch in September 2015. Once the operator makes the subjective decision that two sensor tracks are associated, a manual procedure is used is implement the association within the system. One of the sensor tracks is first promoted to be a system track (by selecting the sensor track and executing the ‘Create System Track’ command) and the second sensor track is then linked to the newly created system track (by selecting the system track and the sensor track and then executing the ‘Add to System Track’ command). The ‘Add to System Track’ command also can be used to associate a sensor track with an existing system track.

One shortcoming of the manual data association process described above is that it is labour-intensive, with operator interaction required both to assess tracks for association and then to carry out the association operation itself. Experience during trials showed that manual association was not feasible in situations involving more than a small number of sensor tracks. In particular, the manual process was not well-suited to the association of UWSS bearing tracks or to situations involving highly-fragmented radar tracks.

Figure 2: *Northern Watch surveillance system display of AIS and radar track histories for HMCS SHAWINIGAN. Individual sensor position reports are indicated as yellow dots. Hovering the mouse over a yellow dot will display the corresponding report's time and position data.*

At a medium level of automation, decision aids provide data association recommendations to the operator, who then makes the decision to either accept or reject the recommendation. The decision aid must provide the operator with the information required to evaluate the system's recommendation. This information may include: the scores used to rank candidate associations; the sensor data, including measures of uncertainty, that are inputs to the association criteria; and related visualizations. At a high level of automation, data association is performed automatically by the system, without the requirement for operator interaction. However, as is the case with semi-automated decision aids, the operator must be provided with the ability to monitor the results of data association; and, if needed, to override the results of automatic processing.

The system operating mode and automation level may also impact where the data association function is deployed in the system—in the Arctic, as part of the ASDS, or in the southern DSCC. A manual data association function almost certainly must be located at the DSCC in order to avoid latencies related to satellite communications. However, for an automated or semi-automated capability, it can be argued that the data association function be located in the ASDS. This would allow all available data to be exploited for association and avoid any restrictions on data type or update rate that might be imposed by satellite bandwidth constraints, if the data association function were to be located in the DSCC. The user interface component of an automated or semi-automated data association capability should be located in the DSCC, to avoid latencies, as in the case of the manual capability.

2.2 A hypothesis test approach to track association

The concepts for semi-automated or automated data association require the use of objective decision criteria for establishing that two or more sensor tracks originate from the same detected

real-world object. This problem, termed track association, has been widely studied in the data fusion literature, as part of the overall data fusion process that includes tracking, classification, situation assessment and resource management. Track association has traditionally been approached from the perspective of statistical decision theory, using a family of related techniques that include maximum likelihood, likelihood ratio, and maximum a posteriori [8][9]. The statistical hypothesis test for track association, which is based on the statistical distribution of the difference between track state estimates, has a long history of use that extends back to the early 1970s [10]. While the track states used for the association tests have traditionally been kinematic estimates of position and/or velocity, these have also been extended to include non-kinematic attributes, such as radar cross-section or emitter characteristics.

As suggested by the name, the statistical hypothesis test approach to track association is based on the hypothesis test from basic statistics [11]. Using the hypothesis test, a *null hypothesis*, H_0, and an *alternative hypothesis*, H_1, are designated. The objective of the hypothesis test is to reject the null hypothesis, based on the values of a test statistic tailored to the distribution of the data. Rejection of the null hypothesis then leads to the acceptance of the alternative hypothesis. While not taking into account all factors considered in more recent techniques, the hypothesis test approach is both well understood and easily implemented, and so represents a good starting point for the application and potential implementation of automated track association to Arctic surveillance.

Prior studies on the application of track association specific to the types of sensors used in Northern Watch have focused primarily on the association of radar and AIS [12][13][14][15]. Garcia et al. [12] describe the transformation of AIS data from geodetic to local coordinates and the use of a hypothesis test similar to that applied in this Scientific Report. Carthel et al. [13] use a distributed multi-hypothesis test algorithm for the association of AIS and radar tracks. The Centurian harbour surveillance testbed described by Bick and Barock [14] is reported to process data from underwater arrays in addition to AIS and radar. However, no technical details are provided on the algorithms used for data association. The more ad-hoc approach employed by Shijun et al. [15] bears some similarity to the gating criteria that are often applied prior to the application of the hypothesis test. The PASSAGES project, described by Battistello et al. [16], has produced a fusion architecture for an array of satellite and ground-based maritime surveillance sensors that include satellite AIS, Long Range Identification and Tracking (LRIT), synthetic aperture radar, ground-based radar, and Electronic Support Measures (ESM). Track association is based on a likelihood ratio test that takes into account both position and velocity criteria.

While relatively little has been reported on the association of underwater acoustic array data with above-water sensor tracks, there is a substantial literature [17][18][19] on the use of the hypothesis test approach for the association of radar and bearings-only ESM tracks that is relevant to the association of UWSS bearings against radar or AIS. What follows is a standard presentation of the statistical hypothesis test approach to track association using kinematic state estimates.

Consider the pair of sensor tracks, X_m^i, the i-th track output by sensor m, and X_n^j, the j-th track output by sensor n. Assume that X_m^i and X_n^j contain estimates $\hat{\mathbf{x}}_m^i(t)$ and $\hat{\mathbf{x}}_n^j(t)$, of the corresponding ground-truth kinematic states $\mathbf{x}_m^i(t)$ and $\mathbf{x}_n^j(t)$, both obtained at time t. Applying the hypothesis test approach to the association of tracks X_m^i and X_n^j, choose as the null hypothesis H_0 that X_m^i and X_n^j originate from the same object, and as the alternative hypothesis H_1 that the

two tracks originate from different objects. These two hypotheses are cast into mathematical form, in terms of the difference $\boldsymbol{\delta}_{m,n}^{i,j}(t) = \mathbf{x}_m^i(t) - \mathbf{x}_n^j(t)$ between the tracks' kinematic states at time *t*:

$$\begin{aligned} H_0&: \mathbf{x}_m^i(t) - \mathbf{x}_n^j(t) = 0; \\ H_1&: \mathbf{x}_m^i(t) - \mathbf{x}_n^j(t) \neq 0. \end{aligned} \tag{1}$$

This is based on the assumption that if the two tracks are estimates of the same underlying object they must also share the same kinematic state. A decision to reject the null hypothesis is therefore a decision that the track state estimates are sufficiently different that the two sensor tracks could not have originated from the same object. If the track state estimates are not sufficiently different to reject the same source hypothesis, then, by default, the tracks are concluded to have originated from the same object.

In formulating the hypothesis test for track association the following assumptions are made regarding the state estimates for X_m^i and X_n^j:

1. The estimates are Gaussian distributed, with means $\hat{\mathbf{x}}_m^i(t)$ and $\hat{\mathbf{x}}_n^j(t)$, and covariances, $\mathbf{P}_m^i(t)$ and $\mathbf{P}_n^j(t)$.

2. State estimates are unbiased.

3. State estimates are obtained at a common time, based on a common coordinate system, and have identical state components and dimensions.

Given that the track state estimates are Gaussian-distributed, $\widehat{\boldsymbol{\delta}}_{n,m}^{i,j}(t)$ will also be Gaussian, with mean $\hat{\mathbf{x}}_m^i(t) - \hat{\mathbf{x}}_n^j(t)$ and covariance $\mathbf{P}_\delta(t)$, where

$$\mathbf{P}_\delta(t) = \mathbf{P}_m^i(t) + \mathbf{P}_n^j(t) - \mathbf{P}_{m,n}^{ij}(t) - \mathbf{P}_{m,n}^{ji}(t). \tag{2}$$

The two terms $\mathbf{P}_{m,n}^{ij}(t)$ and $\mathbf{P}_{m.n}^{ji}(t)$ represent the cross-covariance between the track state estimates for X_m^i and X_n^j. In general, the cross-covariance is required to be taken into consideration. This is true where track state estimates result from the application of a filtering algorithm, as it has been shown that tracks originating from the same source will become correlated by common process noise [20].

The decision to accept or reject the null hypothesis is based on a test statistic calculated on $\widehat{\boldsymbol{\delta}}_{n,m}^{i,j}(t)$. The quantity $D\left(\widehat{\boldsymbol{\delta}}_{n,m}^{i,j}(t)\right)$, defined as

$$D\left(\widehat{\boldsymbol{\delta}}_{n,m}^{i,j}(t)\right) = \left(\hat{\mathbf{x}}_m^i(t) - \hat{\mathbf{x}}_n^j(t)\right)^T \mathbf{P}_\delta(t)^{-1}\left(\hat{\mathbf{x}}_m^i(t) - \hat{\mathbf{x}}_n^j(t)\right) \tag{3}$$

or equivalently

$$D\left(\widehat{\boldsymbol{\delta}}_{n,m}^{i,j}(t)\right) = \widehat{\boldsymbol{\delta}}_{n,m}^{i,j}(t)^T \mathbf{P}_{\delta}(t)^{-1} \widehat{\boldsymbol{\delta}}_{n,m}^{i,j}(t), \tag{4}$$

has a χ^2 distribution with *s* degrees of freedom for Gaussian-distributed track state differences, where *s* is the dimension of the track state difference. $D\left(\widehat{\boldsymbol{\delta}}_{n,m}^{i,j}(t)\right)$ is widely used in the data fusion literature and is known by multiple names including "normalised distance squared", "statistical distance" or "chi-squared distance". In this Scientific Report the term statistical distance will be used. The null hypothesis is rejected if $D\left(\widehat{\boldsymbol{\delta}}_{n,m}^{i,j}(t)\right)$exceeds the threshold distance $d(s,\alpha)$, where $d(s,\alpha)$ is defined by the expression

$$\int_0^{d(s,\alpha)} \chi_s^2\,(x)dx = 1 - \alpha, \tag{5}$$

and the *level of significance*, α, of the hypothesis test is the probability of rejecting a null hypothesis that is true.

If the null hypothesis is rejected, it is concluded that sensor tracks X_m^i and X_n^j are not associated. Otherwise, if $D\left(\widehat{\boldsymbol{\delta}}_{n,m}^{i,j}(t)\right) \leq d(s,\alpha)$, the null hypothesis is accepted and it is assumed that sensor tracks X_m^i and X_n^j are associated. In cases where multiple tracks satisfy the association criteria, the statistical distance is also used as a measure for ranking competing track-to-track associations [8][9].

In order to simplify the notation, the time index *t* will be dropped when discussing the association of tracks based on state estimates obtained at a single instant in time. Also, superscripts designating specific tracks will be dropped in cases where track identifiers are not relevant. For example, the statistical distance between track state estimates from sensor *m* and sensor *n*, without reference to a specific time or track identifiers, will be denoted by $D\left(\widehat{\boldsymbol{\delta}}_{m,n}\right)$.

3 Association tests for Northern Watch tracks: Theoretical development

In this section, the hypothesis test described in Section 2.2 is applied to the association of track data produced by the Northern Watch sensors. The hypothesis test provides an objective measure for deciding whether a pair of sensor tracks originates from the same detected object. It is used to formulate data association tests between sensor tracks of the following types:

- one dimensional (1D) bearing estimates representative of an UWSS bearing report
- two dimensional (2D) position estimates representative of a UWSS cross-fix report
- two dimensional (2D) position estimates representative of information derived from an AIS position report
- two dimensional (2D) polar (range, bearing) position estimates representative of a radar track report

Each of these sensor track types are described in greater detail in Section 3.1.

Two approaches to hypothesis test-based track association are considered. The first approach, presented in Section 3.2, is a single report test that provides a criterion for making association decisions based on a single set of reports from a pair of sensor tracks, calculated at a single instant in time. The second approach, presented in Section 3.3, uses a cumulative, multiple report test that provides a criterion for making an association decision based on multiple sets of state estimates from a pair of sensor tracks, collected over an extended time interval.

In Section 4 the hypothesis test approach is demonstrated using simulated data.

3.1 Sensor track models

This section describes models for the AIS, radar, and UWSS track types used in the formulation of track association test criteria and in subsequent testing using simulated data. In order to limit the scope of the study, the following assumptions have been made:

1. Sensor track reports being tested for association have identical time stamps. In reality, individual sensors report asynchronously and data from two sensors will not normally be time aligned. In such a case, the data from one sensor must be projected forward or backward to a time coincident with that of the data from the other sensor.

2. Sensor track reports are referenced to a common time source. In the Northern Watch system, all sensors derive their time from a Network Time Protocol (NTP) server. In general, however, data from individual sensors may be time-stamped with respect to local clocks which are not synchronized (or worse yet, may not be time-stamped at all).

3. Sensor track reports are referenced to a common coordinate system. In reality, individual sensor coordinate systems will not be precisely aligned and sensor registration processes are required to determine the appropriate transformations to a common coordinate system.

4. Association tests are limited to position or bearing data. Other data types that may be applicable to determining the association between sensor reports, including velocity, bearing rate and attribute data, are not exploited.

5. Track state estimates of position or bearing are unbiased and Gaussian-distributed.

6. Sensor tracks are based on simulated tracker outputs, generated by perturbing ground truth positions (or bearings) with additive Gaussian noise. This allows for a simplification of the hypothesis test, as individual track reports are uncorrelated and there is no process noise. Hence, the cross-covariance between state estimates in Equation (2) can be ignored.

7. Sensor tracks are continuous and there are no false tracks (i.e., the probability of detection is 1.0 and the probability of false alarm is 0.0).

8. A local Cartesian (x, y) coordinate system is used for 2D position reports rather than the geodetic (latitude, longitude) coordinates used by the real Northern Watch sensors. Association tests are based on 2D position or bearing data in a Cartesian coordinate system tangent to the Earth's surface. The origin of the coordinate system is assumed to be coincident with the reference point for bearings-only data from one of the underwater array.

9. First-order estimates are used for non-linear transformations of Gaussian-distributed state estimates (i.e., means and covariances) [21]. These estimates are required in the derivation of positional cross-fixes from multiple bearing measurements and in the transformation between polar and Cartesian coordinate systems. Given a transformation $\mathbf{y} = \mathbf{g}(\mathbf{x})$ of the random vector $\mathbf{x}$, the first-order estimates of the mean and covariance of $\mathbf{y}$ are defined as

$$\hat{\mathbf{y}} \approx \mathbf{g}(\hat{\mathbf{x}}) \tag{6}$$

and

$$\mathbf{P}_y \approx \left.\frac{\partial \mathbf{g}(\mathbf{x})}{\partial \mathbf{x}}\right|_{\mathbf{x}=\hat{\mathbf{x}}} \mathbf{P}_x \left(\left.\frac{\partial \mathbf{g}(\mathbf{x})}{\partial \mathbf{x}}\right|_{\mathbf{x}=\hat{\mathbf{x}}}\right)^{\boldsymbol{T}} \tag{7}$$

where $\hat{\mathbf{x}}$ and $\mathbf{P}_x$ are the mean and covariance of $\mathbf{x}$, respectively. The term $\partial \mathbf{g}(\mathbf{x}) / \partial \mathbf{x}$ is the matrix of partial derivatives of the transformation, also termed the Jacobian. First-order estimates have been applied to the estimation of dynamic non-linear systems; for example, with use in the Extended Kalman Filter [22].

10. An idealised model of the underwater arrays is used that, for example, ignores depth / elevation angle and left/right ambiguity. The model for the arrays is discussed in more detail in Section 3.1.3.

3.1.1 Automatic Identification System (AIS)

The AIS reports that are broadcast by vessels at sea include position data, in latitude and longitude, and velocity data, in course and speed, as part of both Class A and Class B AIS Position Report messages [23][24]. AIS provides limited information as to the uncertainty in contact position. The binary-valued Position Accuracy field, in the AIS Position Report message, indicates whether position accuracy is high (≤ 10 m) or low (> 10 m). No uncertainty data are provided for AIS contact course and speed. Position Reports are broadcast every 2 to 10 s when a vessel is underway. In the Northern Watch system, AIS reports are time-stamped when they are input from the AIS receiver.

For the purpose of this study, AIS position data, in latitude and longitude, are assumed to have been transformed into 2D Cartesian (x, y) values relative to a specified system reference point. An AIS position estimate for a contact at time t is represented as $\hat{\mathbf{x}}_{AIS}(t) = [\hat{x}, \hat{y}]^T$. It is assumed that the uncertainty in AIS position estimates can be expressed as a circular area of uncertainty of radius σ_{AIS}, whose value is based on the value of the Position Accuracy field. σ_{AIS} is assumed to be a constant, independent of time.[2] AIS position estimates are therefore assumed to have an associated covariance $\mathbf{P}_{AIS} = \begin{bmatrix} \sigma_{AIS}^2 & 0 \\ 0 & \sigma_{AIS}^2 \end{bmatrix}$.

In certain instances, it can also be useful to represent AIS position reports in the form of an equivalent range and bearing relative to a specified reference point (x_A, y_A). An equivalent AIS bearing is used for testing the association of UWSS bearings against AIS position reports. Expressions for the equivalent AIS bearing are developed in Section 3.2.4.

3.1.2 Radar

For the purpose of this study, radar track reports are assumed to consist of estimates of contact range, r, and bearing, β, together with associated variances, σ_r^2 and σ_β^2. Variances in range and bearing are assumed to be uncorrelated and to be constant for a given radar.

In vector form, a radar position report for a contact at time t is expressed as $\hat{\mathbf{x}}_{RDR}(t) = \left[\hat{r}, \hat{\beta}\right]^T$, with an associated covariance $\mathbf{P}_{RDR} = \begin{bmatrix} \sigma_r^2 & 0 \\ 0 & \sigma_\beta^2 \end{bmatrix}$.

Radar reports are converted from polar to Cartesian form using the transformation

$$(x, y) = \mathbf{f}(r, \beta) = (x_R + r\cos\beta, y_R + r\sin\beta), \tag{8}$$

where (x_R, y_R) is the position of the radar in the local coordinate system. Note that in the case of real radar data from the Northern Watch system, polar position reports are referenced to the radar's geodetic latitude and longitude.

[2] Because the AIS Position Accuracy field may have one of two possible values— "high" and "low"—the variance in AIS position may differ between vessels and, at least in theory, could vary over time for a given vessel.

In Cartesian coordinates, the first-order estimate of radar position, $\hat{\mathbf{x}}_{RDR(x,y)} = [\hat{x}, \hat{y}]^T$, is the polar-to-Cartesian transformation of the polar position estimate, given by

$$\hat{\mathbf{x}}_{RDR(xy)} \approx \mathbf{f}(\hat{\mathbf{x}}_{RDR}) = \left[x_R + \hat{r}\cos\hat{\beta}\,, y_R + \hat{r}\sin\hat{\beta}\right]^T. \tag{9}$$

Applying Equation (7), the first-order estimate of covariance $\mathbf{P}_{RDR(xy)}$is then

$$\mathbf{P}_{RDR(xy)} \approx \frac{\partial \mathbf{f}}{\partial \mathbf{x}_{RDR}}(\hat{r}, \hat{\beta}) \begin{bmatrix} \sigma_r^2 & 0 \\ 0 & \sigma_\beta^2 \end{bmatrix} \left(\frac{\partial \mathbf{f}}{\partial \mathbf{x}_{RDR}}(\hat{r}, \hat{\beta})\right)^T, \tag{10}$$

where $\partial \mathbf{f} / \partial \mathbf{x}_{RDR}\,(\hat{r}, \hat{\beta})$, the Jacobian of the polar-to-Cartesian transformation evaluated at the polar position estimate, is

$$\frac{\partial \mathbf{f}}{\partial \mathbf{x}_{RDR}}(\hat{r}, \hat{\beta}) = \begin{bmatrix} \frac{\partial x}{\partial r}(\hat{r}, \hat{\beta}) & \frac{\partial x}{\partial \beta}(\hat{r}, \hat{\beta}) \\ \frac{\partial y}{\partial r}(\hat{r}, \hat{\beta}) & \frac{\partial y}{\partial \beta}(\hat{r}, \hat{\beta}) \end{bmatrix} = \begin{bmatrix} \cos\hat{\beta} & -\hat{r}\sin\hat{\beta} \\ \sin\hat{\beta} & \hat{r}\cos\hat{\beta} \end{bmatrix}. \tag{11}$$

Whereas the variances in range and bearing are assumed to be uncorrelated and constant, the transformation to Cartesian coordinates results in a covariance whose values are both correlated and position-dependent.

3.1.3 UWSS bearing

UWSS bearing reports are generated by bottom-mounted horizontal linear arrays of acoustic sensors. In comparison with other bearings-only sensors, underwater acoustic arrays produce a more complex measurement. Linear underwater acoustic arrays have response functions, also known as beams, in the shape of conic sections aligned with the axis of the array. The bearings measured by the array are the angles between the axis of the array and cone-shaped directional beams, hence the term ‘conical bearing’. Given a bottom-mounted array and a surface contact, the conical angle measured by the array generally will not be equal to the horizontal bearing to the contact (measured relative to the axis of the array) as measured on the surface, as the conical angle will have both horizontal and a vertical components. In addition, because the cone-shaped beams have two intersections with the plane of the surface, a detected signal will appear on both sides of the array, a condition that is termed ‘left/right ambiguity’. Detailed descriptions of underwater acoustic array theory and technology are available in references such as [25].

For the purpose of this study, both idealised arrays and array geometry are assumed as follows:

- The acoustic centres of array *A* and array *B* are located at 2D Cartesian coordinates (0,0) and (0, *d*), respectively, in the local coordinate system.
- Both arrays are linear and are oriented parallel to the *x* axis.
- Bearing angles are measured counter-clockwise relative to the *x* axis.

- The vertical component of the conical angle is ignored; equivalently, the conical angle is assumed to be equal to the horizontal bearing. For detected maritime surface contacts, this is equivalent to placing the arrays at the surface.
- Direct path propagation of acoustic energy is assumed between the detected object and the underwater array. Multipath propagation is not considered.
- Left/right ambiguity is ignored. Contacts are detected only on their true bearing.

The array geometry is illustrated in Figure 3.

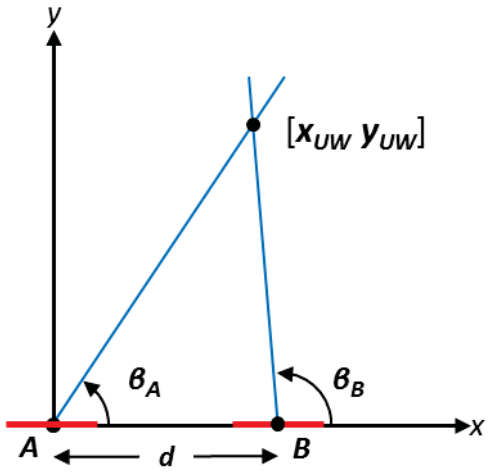

Figure 3: *Array geometry. Arrays A and B (represented by red bars) are positioned at coordinates (0,0) and (0, d), respectively, and are both aligned with the x-axis. Bearing measurements are counter-clockwise relative to the x-axis. A position estimate* $[x_{UW},y_{UW}]$ *is produced from the cross-fixing of bearings* β_A *and* β_B *from the two arrays.*

UWSS bearing reports are assumed to consist of estimates of contact bearing, $\hat{\beta}_{UW}(t)$, referenced to (x_U, y_U), the 2D Cartesian (x, y) location of the acoustic center of the UWSS array; and, an associated bearing variance $\sigma^2_{\beta_{UW}}$. The bearing variance is modelled as a function of conical angle, consistent with the variation in the array beam width computed in [26] and illustrated in Figure 4. The minimum and maximum bearing variances occur at directions perpendicular and parallel to the axis of the array, respectively.

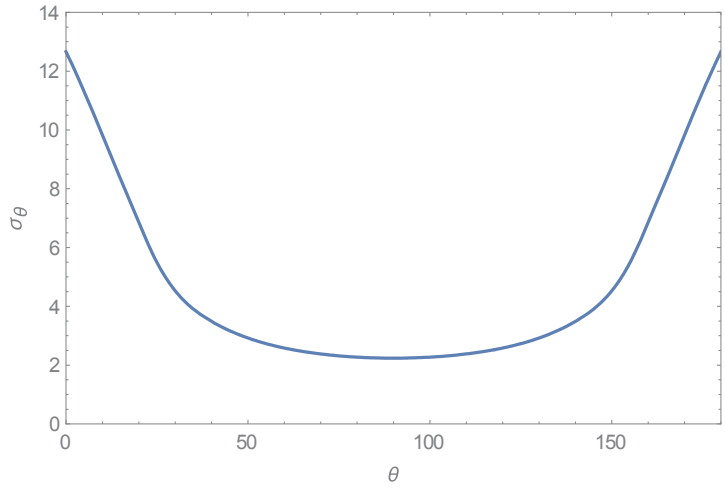

Figure 4: *UWSS bearing variance σ_θ as a function of conical angle θ. This function is based on an interpolation of the beam width values computed in the Northern Watch UWSS operating concept [26].*

3.1.4 UWSS cross-fix

A UWSS 2D Cartesian position estimate for a contact at time t, is based on the cross-fixing of bearing measurements from UWSS arrays A and B, and has the form $\hat{\mathbf{x}}_{UW}(t) = [\hat{x}_{UW}, \hat{y}_{UW}]^T$, with an associated covariance $\mathbf{P}_{UW}(t) = \begin{bmatrix} \sigma_x^2 & \sigma_{xy} \\ \sigma_{xy} & \sigma_y^2 \end{bmatrix}$.

As depicted in Figure 3, the cross-fix position $\mathbf{x}_{UW}$ is a function of the bearing measurements β_A and β_B from UWSS arrays A and B, and the distance d separating the acoustic centers of the two arrays. Making the assumption that the acoustic centres of arrays A and B are located at coordinates (0,0) and (0, d), the cross-fix position is given by

$$\mathbf{x}_{UW} = \mathbf{g}(\beta_A, \beta_B) = \left[\frac{d \sin\beta_B \cos\beta_A}{\sin(\beta_B - \beta_A)}, \frac{d \sin\beta_B \sin\beta_A}{\sin(\beta_B - \beta_A)}\right]^T. \tag{12}$$

The first-order estimate of the cross-fix position is therefore

$$\hat{\mathbf{x}}_{UW}(t) \approx \mathbf{g}(\hat{\beta}_A, \hat{\beta}_B) = \left[\frac{d \sin\hat{\beta}_B \cos\hat{\beta}_A}{\sin(\hat{\beta}_B - \hat{\beta}_A)} \quad \frac{d \sin\hat{\beta}_B \sin\hat{\beta}_A}{\sin(\hat{\beta}_B - \hat{\beta}_A)}\right]^T \tag{13}$$

Applying Equation (7), the first-order estimate of covariance $\mathbf{P}_{UW}$ is specified as

$$\mathbf{P}_{UW} \approx \frac{\partial \mathbf{g}}{\partial(\beta_A, \beta_B)}(\hat{\beta}_A, \hat{\beta}_B) \begin{bmatrix} \sigma_{\beta_A}^2 & 0 \\ 0 & \sigma_{\beta_B}^2 \end{bmatrix} \left(\frac{\partial \mathbf{g}}{\partial(\beta_A, \beta_B)}(\hat{\beta}_A, \hat{\beta}_B)\right)^T, \tag{14}$$

where $\partial \mathbf{g} / \partial(\beta_A, \beta_B)\,(\hat{\beta}_A, \hat{\beta}_B)$, the Jacobian of the cross-fix transformation evaluated at the array bearing estimates, are

$$\frac{\partial \mathbf{g}}{\partial(\beta_A,\beta_B)}(\hat{\beta}_A,\hat{\beta}_B) = \begin{bmatrix} \frac{\partial x_{UW}}{\partial \beta_A}(\hat{\beta}_A,\hat{\beta}_B) & \frac{\partial x_{UW}}{\partial \beta_B}(\hat{\beta}_A,\hat{\beta}_B) \\ \frac{\partial y_{UW}}{\partial \beta_A}(\hat{\beta}_A,\hat{\beta}_B) & \frac{\partial y_{UW}}{\partial \beta_B}(\hat{\beta}_A,\hat{\beta}_B) \end{bmatrix}. \tag{15}$$

The individual elements of $\frac{\partial \mathbf{g}}{\partial(\beta_A,\beta_B)}(\hat{\beta}_A,\hat{\beta}_B)$ are computed as follows:

$$\frac{\partial x_{UW}}{\partial \beta_A}(\hat{\beta}_A,\hat{\beta}_B) = \frac{d\cos\hat{\beta}_B \sin\hat{\beta}_B}{\sin^2(\hat{\beta}_B - \hat{\beta}_A)}; \tag{16}$$

$$\frac{\partial x_{UW}}{\partial \beta_B}(\hat{\beta}_A,\hat{\beta}_B) = -\frac{d\cos\hat{\beta}_A \sin\hat{\beta}_A}{\sin^2(\hat{\beta}_B - \hat{\beta}_A)}; \tag{17}$$

$$\frac{\partial y_{UW}}{\partial \beta_A}(\hat{\beta}_A,\hat{\beta}_B) = \frac{d\sin^2\hat{\beta}_B}{\sin^2(\hat{\beta}_B - \hat{\beta}_A)}; \tag{18}$$

$$\frac{\partial y_{UW}}{\partial \beta_B}(\hat{\beta}_A,\hat{\beta}_B) = -\frac{d\sin^2\hat{\beta}_A}{\sin^2(\hat{\beta}_B - \hat{\beta}_A)}. \tag{19}$$

Two assumptions with regard to the formation of cross-fixes are:

- Bearings from the two arrays are measured at identical times. Otherwise, one or both bearing must be projected backwards or forwards in time to a common time value.
- A separate association mechanism has been used to ascertain that the bearing measurements from the two arrays originate from the same detected object. Frequency information is commonly used for this purpose in the case of narrowband bearings.

3.2 Single report association tests

Using the hypothesis test approach to track-to-track data association introduced in Section 2.2, this section presents the formulation of association test criteria that can be applied to a single pair of track reports from two sensors, computed at one instant in time. The term "single report" association test is used to distinguish these test criteria from tests based on multiple sets of track reports collected over an extended time period. Single report association tests are presented for the following combinations of track report types:

- AIS position reports and radar position reports (Section 3.2.1)
- AIS position reports and UWSS cross-fix reports (Section 3.2.2)
- radar position reports and UWSS cross-fix reports (Section 3.2.3)

- AIS position reports and UWSS bearing reports (Section 3.2.4)
- radar position reports and UWSS bearing reports (Section 3.2.5)

Each of the above tests are based on classical treatments of the statistical distance from sources such as [8][9]. Tests involving bearing reports are similar to those used for the association of bearing-only ESM tracks in [17][18][19].

The UWSS bearing association tests discussed in Sections 3.2.4 and 3.2.5 are formulated for a single UWSS bearing obtained from either one of the two arrays. Section 3.2.6 extends those tests to consider the association of pairs of bearings from both arrays.

One assumption of the hypothesis test, stated in Section 2.2, is that the tracks being tested for association have state estimates with identical track state components. The Northern Watch sensor tracks do not satisfy this assumption, as they include three different types of kinematic state estimates: 1D UWSS bearing; 2D polar (range, bearing) radar position; and 2D Cartesian (*x, y*) UWSS cross-fix and AIS position. In order to test tracks with non-identical state components, one is required to transform one (or both states) to make the state components for both tracks congruent. In the case of sensor track states of differing dimensionality, and where the sensor reports share one or more common dimensions, the report with the higher number of dimensions will be converted into a report of the type matching the report with the lower number of dimensions. For example, before testing for association between radar (range, bearing) and UWSS bearing reports, the radar (range, bearing) report is converted into an equivalent bearing report by selecting the radar report's bearing component.

3.2.1 AIS to radar position report association test

This section presents a criterion, based on the statistical distance, for testing the association between AIS and radar position reports. The statistical distance can be formulated using either Cartesian coordinates or polar coordinates; what follows is the formulation in Cartesian coordinates.

Assume a 2D polar radar position estimate, $\hat{\mathbf{x}}_{RDR} = [\hat{r}, \hat{\beta}]^T$, and a 2D Cartesian AIS position estimate, $\hat{\mathbf{x}}_{AIS}$, together with their corresponding covariances $\mathbf{P}_{RDR}$ and $\mathbf{P}_{AIS}$. Because the radar and AIS tracks have differing coordinate types, $\hat{\mathbf{x}}_{RDR}$ and $\mathbf{P}_{RDR}$ are transformed to an equivalent Cartesian radar position estimate $\hat{\mathbf{x}}_{RDR(xy)}$ and covariance $\mathbf{P}_{RDR\,(xy)}$ before the statistical distance is applied. As described in Section 3.1.2, to first order

$$\hat{\mathbf{x}}_{Rdr\,(xy)} = \begin{bmatrix} \hat{r}\sin\hat{\beta} + x_R \\ \hat{r}\cos\hat{\beta} + y_R \end{bmatrix}, \tag{20}$$

where (x_R, y_R) are the coordinates of the radar relative to the system reference point, and

$$\mathbf{P}_{RDR\,(xy)} = \begin{bmatrix} \sin\hat{\beta} & \hat{r}\cos\hat{\beta} \\ \cos\hat{\beta} & -\hat{r}\sin\hat{\beta} \end{bmatrix} \mathbf{P}_{RDR} \begin{bmatrix} \sin\hat{\beta} & \hat{r}\cos\hat{\beta} \\ \cos\hat{\beta} & -\hat{r}\sin\hat{\beta} \end{bmatrix}^T. \tag{21}$$

Given the AIS position estimate $\hat{\mathbf{x}}_{AIS}$, the Cartesian radar position estimate $\hat{\mathbf{x}}_{RDR(xy)}$, and their associated covariances, the statistical distance $D\left(\widehat{\boldsymbol{\delta}}_{AIS,RDR(xy)}\right)$ is specified as

$$D\left(\widehat{\boldsymbol{\delta}}_{AIS,RDR(xy)}\right) = \left(\hat{\mathbf{x}}_{AIS} - \hat{\mathbf{x}}_{RDR(xy)}\right)^T \left(\mathbf{P}_{AIS} + \mathbf{P}_{RDR(xy)}\right)^{-1} \left(\hat{\mathbf{x}}_{AIS} - \hat{\mathbf{x}}_{RDR(xy)}\right) \tag{22}$$

and has a χ^2 distribution with 2 degrees of freedom.

Alternatively, one can formulate the statistical distance in polar coordinates, by first converting the AIS position estimate and covariance into the polar form, $\hat{\mathbf{x}}_{AIS(r,\beta)}$ and $\mathbf{P}_{AIS(r,\beta)}$, relative to the radar's location, and then comparing these against the radar polar position estimate and covariance, $\hat{\mathbf{x}}_{RDR}$ and $\mathbf{P}_{RDR}$. This approach is used for calculating AIS to radar position associations using collected trials data, as described in [4].

3.2.2 AIS position report to UWSS cross-fix report association test

This section presents a criterion, based on the statistical distance, for testing the association between an AIS position report and a UWSS cross-fix. The statistical measure is effectively the same as the Cartesian form of the statistical distance presented in the previous section for testing the association between AIS and radar position reports.

Given the Cartesian AIS position estimate, $\hat{\mathbf{x}}_{AIS}$, and UWSS cross-fix position estimate, $\hat{\mathbf{x}}_{UW}$, the statistical distance $D\left(\widehat{\boldsymbol{\delta}}_{AIS,UW}\right)$ is given by

$$D\left(\widehat{\boldsymbol{\delta}}_{AIS,UW}\right) = (\hat{\mathbf{x}}_{AIS} - \hat{\mathbf{x}}_{UW})^T (\mathbf{P}_{AIS} + \mathbf{P}_{UW})^{-1} (\hat{\mathbf{x}}_{AIS} - \hat{\mathbf{x}}_{UW}) \tag{23}$$

where the covariances of $\hat{\mathbf{x}}_{AIS}$ and $\hat{\mathbf{x}}_{UW}$ are $\mathbf{P}_{AIS}$ and $\mathbf{P}_{UW}$, respectively.

$D\left(\widehat{\boldsymbol{\delta}}_{AIS,UW}\right)$ has a χ^2 distribution with 2 degrees of freedom.

3.2.3 Radar position report to UWSS cross-fix report association test

This section presents a criterion, based on the statistical distance, for testing the association between a polar radar position estimate, given as a range and bearing, and a UWSS cross-fix.

Consider the 2D polar radar position estimate, $\hat{\mathbf{x}}_{RDR}$, and the 2D Cartesian UWSS cross-fix position estimate, $\hat{\mathbf{x}}_{UW}$, together with their corresponding covariances $\mathbf{P}_{RDR}$ and $\mathbf{P}_{UW}$. Using the approach described in Section 3.2.1, the polar radar position estimate and covariance are first converted into Cartesian form, as $\hat{\mathbf{x}}_{RDR(xy)}$ and $\mathbf{P}_{RDR(xy)}$, using Equations (20) and (21), respectively. The statistical distance $D\left(\widehat{\boldsymbol{\delta}}_{RDR(xy),UW}\right)$ is given by

$$D\left(\widehat{\boldsymbol{\delta}}_{RDR(xy),UW}\right) = \left(\hat{\mathbf{x}}_{RDR\,(xy)} - \hat{\mathbf{x}}_{UW}\right)\left(\mathbf{P}_{RDR\,(xy)} + \mathbf{P}_{UW}\right)^{-1} \left(\hat{\mathbf{x}}_{RDR\,(xy)} - \hat{\mathbf{x}}_{UW}\right)^T \tag{24}$$

$D\left(\widehat{\boldsymbol{\delta}}_{RDR(xy),UW}\right)$ has a χ^2 distribution with 2 degrees of freedom.

Alternatively, one could formulate the statistical distance in polar coordinates, by first converting the UWSS cross-fix position estimate and covariance into the polar form, $\hat{\mathbf{x}}_{UW(r,\beta)}$ and $\mathbf{P}_{UW(r,\beta)}$, relative to the radar's location, and then comparing them against the radar polar position estimate and covariance, $\hat{\mathbf{x}}_{RDR}$ and $\mathbf{P}_{RDR}$.

3.2.4 AIS position report to UWSS bearing report association test

This section presents a criterion, based on the statistical distance, for testing the association between an AIS position estimate and a UWSS bearing estimate.

Consider the AIS position estimate, $\hat{\mathbf{x}}_{AIS} = [\hat{x}, \hat{y}]^T$, and the UWSS bearing estimate, $\hat{\beta}_{UW}$. As the AIS and UWSS track types have differing dimensionality and coordinate types, the track with the higher number of dimensions (AIS position) is first transformed into a track type matching the track with the lower number of dimensions (UWSS bearing) before the statistical distance is applied.

An equivalent AIS bearing, $\hat{\beta}_{AIS}$, is computed from $\hat{\mathbf{x}}_{AIS}$ using the transformation

$$\beta_{AIS} = f_{\beta}(\mathbf{x}_{AIS}) = \tan^{-1}\left(\frac{x - x_U}{y - y_U}\right), \tag{25}$$

where (x_U, y_U) is the position of the acoustic center of the array. To first-order,

$$\hat{\beta}_{AIS} \approx f_{\boldsymbol{\beta}}(\hat{\mathbf{x}}_{AIS}) = \tan^{-1}\left(\frac{\hat{x} - x_{UW}}{\hat{y} - y_{UW}}\right), \tag{26}$$

Applying Equation (7), the first-order estimate of the variance of the AIS bearing estimate, $\sigma^2_{\hat{\beta}_{AIS}}$, is

$$\sigma^2_{\hat{\beta}_{AIS}} \approx \frac{\partial \beta_{AIS}}{\partial \mathbf{x}_{AIS}}(\hat{x}, \hat{y}) \mathbf{P}_{AIS} \left(\frac{\partial \beta_{AIS}}{\partial \mathbf{x}_{AIS}}(\hat{x}, \hat{y})\right)^T, \tag{27}$$

where the expression for $\frac{\partial \beta_{AIS}}{\partial \mathbf{x}_{AIS}}(\hat{x}, \hat{y})$, the Jacobian of the Cartesian-to-bearing transformation, evaluated at the value of the AIS position estimate, is given by

$$\frac{\partial \beta_{AIS}}{\partial \mathbf{x}_{AIS}}(\hat{x}, \hat{y}) = \left[\frac{-\hat{y}}{\hat{x}^2 + \hat{y}^2} \quad \frac{\hat{x}}{\hat{x}^2 + \hat{y}^2}\right]. \tag{28}$$

Given that $\mathbf{P}_{AIS}$ is a diagonal matrix of the form $\begin{bmatrix} \sigma^2_{AIS} & 0 \\ 0 & \sigma^2_{AIS} \end{bmatrix}$, Equation (27) can be further simplified, with the result

$$\sigma^2_{\hat{\beta}_{AIS}} \approx \frac{\sigma^2_{AIS}}{\hat{x}^2+\hat{y}^2}. \tag{29}$$

The statistical distance $D\left(\hat{\delta}_{AIS(\beta),UW(\beta)}\right)$ between the AIS bearing $\hat{\beta}_{AIS}$ and UWSS bearing $\hat{\beta}_{UW}$ is then given by

$$D\left(\hat{\delta}_{AIS(\beta),UW(\beta)}\right) = \left(\hat{\beta}_{UW} - \hat{\beta}_{AIS}\right)^2 / \left(\sigma^2_{\hat{\beta}_{UW}} + \sigma^2_{\hat{\beta}_{AIS}}\right). \tag{30}$$

$D\left(\hat{\delta}_{AIS(\beta),UW(\beta)}\right)$ has a χ^2 distribution with 1 degree of freedom.

3.2.5 Radar position report to UWSS bearing report association test

This section presents a criterion, based on the statistical distance, for testing the association of a 2D polar radar position estimate, given as range and bearing, with a UWSS bearing estimate.

Given a radar bearing estimate, $\hat{\beta}_{RDR}$, and a UWSS bearing estimate, $\hat{\beta}_{UW}$, and making the assumption that radar location is coincident with the acoustic center of the array, the statistical distance $D\left(\hat{\delta}_{RDR(\beta),UW(\beta)}\right)$ is

$$D\left(\hat{\delta}_{RDR(\beta),UW(\beta)}\right) = \left(\hat{\beta}_{RDR} - \hat{\beta}_{UW}\right)^2 / \left(\sigma^2_{\hat{\beta}_{RDR}} + \sigma^2_{\hat{\beta}_{UW}}\right). \tag{31}$$

where the variances in $\hat{\beta}_{RDR}$ and $\hat{\beta}_{UW}$ are $\sigma^2_{\hat{\beta}_{RDR}}$ and $\sigma^2_{\hat{\beta}_{UW}}$, respectively.

$D\left(\hat{\delta}_{RDR(\beta),UW(\beta)}\right)$ has a χ^2 distribution with 1 degree of freedom.

If the radar location is not coincident with the acoustic center of the array, it is first necessary to transform the radar position report to Cartesian form and then compute an equivalent radar bearing that is referenced to the acoustic center of the array (essentially the same procedure used to calculate an equivalent AIS bearing in Section 3.2.4). This procedure was required for the analysis of experimental trials data as described in [4].

3.2.6 Association tests using UWSS bearing pairs

Sections 3.2.4 and 3.2.5 present criteria for testing the association between a single UWSS bearing and a Cartesian XY position report (Section 3.2.4) or a polar (range, bearing) position report (Section 3.2.5). However, the Northern Watch system employs two underwater arrays. What is an appropriate association test for use when an object is detected simultaneously on two arrays? This question is particularly pertinent to the comparison between association tests using UWSS bearings and UWSS cross-fixes.

Consider, for example, the AIS position estimate, $\hat{\mathbf{x}}_{AIS}$, and the two bearing estimates, $\hat{\beta}_A$ and $\hat{\beta}_B$, from array *A* and array *B*. One option is to formulate a two-array test as the logical intersection of

the two single array tests, between $\hat{\beta}_A$ and $\hat{\mathbf{x}}_{AIS}$ and between $\hat{\beta}_B$ and $\hat{\mathbf{x}}_{AIS}$, using the statistical distance $D\left(\hat{\delta}_{AIS(\beta),UW(\beta)}\right)$ described in Section 3.2.4. In simple terms, the two-array test is accepted if both of the single array tests are accepted . One negative of this approach is that the two-array test will have a lower significance relative to the significance of the individual single array tests (because the test is now rejected if either of the two single array tests is rejected). This is demonstrated in Section 4.2.

An alternative option is to use a single test based on the combination of bearing difference estimates from both arrays. Again, consider the AIS position estimate, $\hat{\mathbf{x}}_{AIS}$, and the two bearing estimates, $\hat{\beta}_A$ and $\hat{\beta}_B$, from array *A* and array *B*. The AIS position estimate is converted to the equivalent AIS bearing estimates, $\hat{\beta}_{AIS(A)}$, relative to the location of array *A*, and $\hat{\beta}_{AIS(B)}$, relative to the location of array *B*. This is done according to the procedure described in Section 3.2.4. The hypothesis test is then based on the two bearing difference estimates, $\hat{\delta}_A = \hat{\beta}_A - \hat{\beta}_{AIS(A)}$ and $\hat{\delta}_B = \hat{\beta}_B - \hat{\beta}_{AIS(B)}$, and their associated covariances. These are represented in vector format as

$$\hat{\boldsymbol{\delta}} = \begin{bmatrix}\hat{\delta}_A & \hat{\delta}_B\end{bmatrix}^T \text{and covariance } \mathbf{P}_\delta = \begin{bmatrix}\sigma^2_{\delta_A} & \sigma_{\delta_A\delta_B} \\ \sigma_{\delta_A\delta_B} & \sigma^2_{\delta_B}\end{bmatrix};$$

where $\sigma^2_{\delta_A} = \sigma^2_{\beta_A} + \sigma^2_{\beta_{AIS(A)}}$ and $\sigma^2_{\delta_B} = \sigma^2_{\beta_B} + \sigma^2_{\beta_{AIS(B)}}$ are the variances of $\hat{\delta}_A$and $\hat{\delta}_B$, respectively, and $\sigma_{\delta_A\delta_B} = E\left[\left(\delta_A - \hat{\delta}_A\right)\left(\delta_B - \hat{\delta}_B\right)\right]$ is the covariance of $\hat{\delta}_A$ and $\hat{\delta}_B$. Note that because $\hat{\delta}_A$ and $\hat{\delta}_B$ are based on a common AIS position estimate, they are not assumed to be independent. The statistical distance then takes the standard form, $D\left(\hat{\boldsymbol{\delta}}\right) = \hat{\boldsymbol{\delta}}^T \mathbf{P}_\delta^{-1} \hat{\boldsymbol{\delta}}$, which has a χ^2 distribution with 2 degrees of freedom. This test will be named the combined bearing association test.

If it is possible to neglect $\sigma_{\delta_A\delta_B}$, $D(\hat{\boldsymbol{\delta}})$ can be re-written in simplified form as

$$\begin{aligned} D\left(\hat{\boldsymbol{\delta}}\right) &= \hat{\delta}_A^2/\sigma^2_{\delta_A} + \hat{\delta}_B^2/\sigma^2_{\delta_B} \\ &= \left(\hat{\beta}_A - \hat{\beta}_{AIS(A)}\right)^2 / \left(\sigma^2_{\beta_A} + \sigma^2_{\beta_{AIS(A)}}\right) \\ &\quad + \left(\hat{\beta}_B - \hat{\beta}_{AIS(B)}\right)^2 / \left(\sigma^2_{\beta_B} + \sigma^2_{\beta_{AIS(B)}}\right) \end{aligned} \tag{32}$$

One consequence of establishing that two UWSS bearings are each associated with a third source is that one can infer that the UWSS bearings are associated with each other. This is an important distinction between the UWSS combined bearing tests and UWSS cross-fix tests. Tests involving UWSS cross-fixes must assume the existence of a separate association process for establishing that the bearing reports detected on the two arrays originate from the same object. The process of testing for associations against a common track from another data source therefore has the potential for use as an aid to establishing intrasensor associations between the large numbers of acoustic bearings that may originate from a single detected object on an individual array.

3.3 Multiple report association test

Using single report tests of the type described in Section 3.2, an association decision is based on track data collected at one instant in time. In general, however, tracks may consist of many reports gathered over an extended period of time and one single report association test may not be sufficient to determine whether or not two tracks are associated. This issue is more likely to arise as the numbers of vessels present in a surveillance area increases, and when bearings-only sensors are involved. For example, ambiguous associations resulting from short-term, spurious, alignments in bearing with multiple vessels are not uncommon for UWSS systems.

One approach is to use single report tests to periodically re-test track associations. However, if the single report association tests are ambiguous this can lead to unstable track-to-track associations that change over time, with a consequent degradation in the overall quality of the surveillance picture. An alternative approach is to base track-to-track association decisions on data gathered from multiple track reports, over an extended period of time. What follows is a simple extension of the single report test, based on the approach used by La Scala and Farina [18] to implement a sliding-window track association algorithm. This approach also has been applied by Gendron [19] for testing the association between radar and ESM tracks.

In Section 2.1, the hypothesis test was presented for assessing the association between tracks X_m^i and X_n^j, given the single pair of state estimates $\hat{\mathbf{x}}_m^i(t)$ and $\hat{\mathbf{x}}_n^j(t)$, obtained at a common time *t*. In theory, one can formulate a similar hypothesis test based on two sequences of l state estimates, $\{\hat{\mathbf{x}}_m^i(t_k)\}$ and $\{\hat{\mathbf{x}}_n^j(t_k)\}$, *k=1,…,l*, from tracks X_m^i and X_n^j, respectively. As in the previous section, it is assumed that the two sequences are perfectly aligned in time. The null hypothesis, H_0, that X_m^i and X_n^j originate from the same platform, can then be recast based on the sequence of track state differences, $\widehat{\boldsymbol{\delta}}_{m,n}^{i,j}(t_k)$, calculated over $\{\hat{\mathbf{x}}_m^i(t_k)\}$ and $\{\hat{\mathbf{x}}_n^j(t_k)\}$, in the form

$$H_0: \boldsymbol{\Delta}_{m,n}^{i,j}(l) = 0; \tag{33}$$

$$H_1: \boldsymbol{\Delta}_{m,n}^{i,j}(l) \neq 0, \tag{34}$$

where the cumulative track state difference $\boldsymbol{\Delta}_{m,n}^{i,j}(l) = \left[\boldsymbol{\delta}_{m,n}^{i,j}(t_1)\middle|\boldsymbol{\delta}_{m,n}^{i,j}(t_2)\middle|\cdots\middle|\boldsymbol{\delta}_{m,n}^{i,j}(t_l)\right]^T$ is the stacked vector of state differences $\boldsymbol{\delta}_{m,n}^{i,j}(t_k)$ and is of dimension $l{\cdot}s$ Given that each of the estimated state differences $\widehat{\boldsymbol{\delta}}_{m,n}^{i,j}(t_k)$ are Gaussian-distributed, the estimated cumulative track state difference, $\widehat{\boldsymbol{\Delta}}_{m,n}^{i,j}(l)$, is also Gaussian, with mean $\left[\widehat{\boldsymbol{\delta}}_{m,n}^{i,j}(t_1)\middle|\widehat{\boldsymbol{\delta}}_{m,n}^{i,j}(t_2)\middle|\cdots\middle|\widehat{\boldsymbol{\delta}}_{m,n}^{i,j}(t_l)\right]^T$ and covariance $\mathbf{P}_\Delta(l)$, of dimension $ls \times ls$. The statistical distance $D(\widehat{\boldsymbol{\Delta}}_{m,n}^{i,j}(l))$ for the estimated cumulative state difference $\widehat{\boldsymbol{\Delta}}_{m,n}^{i,j}(l)$ takes the standard form $D\left(\widehat{\boldsymbol{\Delta}}_{m,n}^{i,j}(l)\right) = \widehat{\boldsymbol{\Delta}}_{m,n}^{i,j}(l)^T \mathbf{P}_\Delta(l)^{-1} \widehat{\boldsymbol{\Delta}}_{m,n}^{i,j}(l)$ and has a χ^2 distribution with $s{\cdot}l$ degrees of freedom.

However, as noted in [27], $\mathbf{P}_\Delta(l)$ is a large matrix, with a complex structure involving diagonal blocks corresponding to $\mathbf{P}_\delta(t_k)$ and off-diagonal blocks corresponding to the cross-covariance between each of the elements of $\{\widehat{\boldsymbol{\delta}}_{m,n}^{i,j}(t_k)\}$, *k=1,…,l*. Consequently, the approach described

above has not been commonly applied. In [18], La Scala and Farina use the simplifying assumption that the cross-covariance between the $\widehat{\boldsymbol{\delta}}_{m,n}^{i,j}(t_k)$ can be neglected, in which case the statistical distance for $\widehat{\boldsymbol{\Delta}}_{m,n}^{i,j}(l)$ is reduced to the sum

$$D\left(\widehat{\boldsymbol{\Delta}}_{m,n}^{i,j}(l)\right) \approx \sum_{k=1}^{l} \widehat{\boldsymbol{\delta}}_{m,n}^{i,j}(t_k)^T \mathbf{P}_{\delta(t_k)}^{-1} \widehat{\boldsymbol{\delta}}_{m,n}^{i,j}(t_k), \tag{35}$$

or equivalently, the sum of the statistical distances at each of the times t_k

$$D\left(\widehat{\boldsymbol{\Delta}}_{m,n}^{i,j}(l)\right) \approx \sum_{k=1}^{l} D\left(\widehat{\boldsymbol{\delta}}_{m,n}^{i,j}(t_k)\right). \tag{36}$$

This assumption comes with the proviso that the distribution of $D(\widehat{\boldsymbol{\Delta}}_{m,n}^{i,j}(l))$ is now only approximately χ^2, which, in turn, means that the threshold values used for association tests are approximations as well. The effect of window length and test significance on test threshold are considered in [28] by La Scala and Farina.

Consider the specific case of a multiple report association test between an AIS track and a UWSS bearing track. Applying the transformation between AIS positions and equivalent bearings (referenced to the array location) described in Section 3.2.4, the association test is computed using the set of UWSS bearing reports $\{\hat{\beta}_{UW}(t_k)\}$ and the set of equivalent AIS bearing reports $\{\hat{\beta}_{AIS}(t_k)\}$. In Equation (30), the statistical distance between AIS bearing $\hat{\beta}_{AIS}(t_k)$ and UWSS bearing $\hat{\beta}_{UW}(t_k)$ is given by

$$D\left(\hat{\delta}_{AIS(\beta),UW(\beta)}(t_k)\right) = \left(\hat{\beta}_{UW}(t_k) - \hat{\beta}_{AIS}(t_k)\right)^2 / \left(\sigma_{\hat{\beta}_{UW}}^2(t_k) + \sigma_{\hat{\beta}_{AIS}}^2(t_k)\right).$$

Substituting this expression into Equation (36), the statistical distance calculated over the set of *l* UWSS and AIS bearing reports is

$$D\left(\widehat{\boldsymbol{\Delta}}_{AIS(\beta),UW(\beta)}(l)\right) \approx \sum_{k=1}^{l} \left(\hat{\beta}_{UW}(t_k) - \hat{\beta}_{AIS}(t_k)\right)^2 / \left(\sigma_{\hat{\beta}_{UW}}^2(t_k) + \sigma_{\hat{\beta}_{AIS}}^2(t_k)\right). \tag{37}$$

$D\left(\widehat{\boldsymbol{\Delta}}_{AIS(\beta),UW(\beta)}(l)\right)$ has a distribution which is approximately χ^2 with *l* degrees of freedom. A demonstration of multiple report association between an AIS track and a UWSS bearing track is provided in Section 4.3.

In practice, how could a multiple report association test be applied? In a real-time mode of operation (i.e., when tracks are being updated in real-time), a sliding-window approach—with the association test based on the last *n* track updates—would have advantages. This would allow for the accumulation of a sufficient number of data samples necessary to make stable, accurate association decisions. In time-critical applications, such as targeting, the length of the sliding window will need to be adjusted to trade-off between association performance and the time latency resulting from the collection of additional data. From the perspective of the remote, unmanned surveillance concept for Northern Watch, with a Southern operator who may only

periodically review the data transmitted from the Arctic, a non-real time mode of operation may be more appropriate. Multiple-report association could be used either in a sliding window mode or in a batch mode that updates track-to-track associations based on all data received since the last operator review. While the selection of window length is not addressed specifically in this study, an analysis of the relationship between window length and association performance should be possible using the approach discussed in [29]. Any latency introduced by windowed or batch processing is not expected to be a significant consideration for non-real time operation.

4 Association tests for Northern Watch tracks: Simulation results

Using simulated data, a series of tests were conducted to demonstrate the single report association tests from Section 3.2 and the multiple report tests from Section 3.3. Test scenarios involve vessel transits through a surveillance region that is representative of the Northern Watch site on Barrow Strait. This is depicted in Figure 5. The coordinate system is oriented with the x-axis pointing west and the y-axis pointing south. For the radar to AIS association tests described in Section 4.1, the radar is assumed to be located at the origin. For the underwater array to AIS association tests discussed in Section 4.2, array *A* and array *B* are located at the origin, and at (5000 m, 0 m), respectively. Otherwise, the array configuration is as assumed in Section 3.1.3.

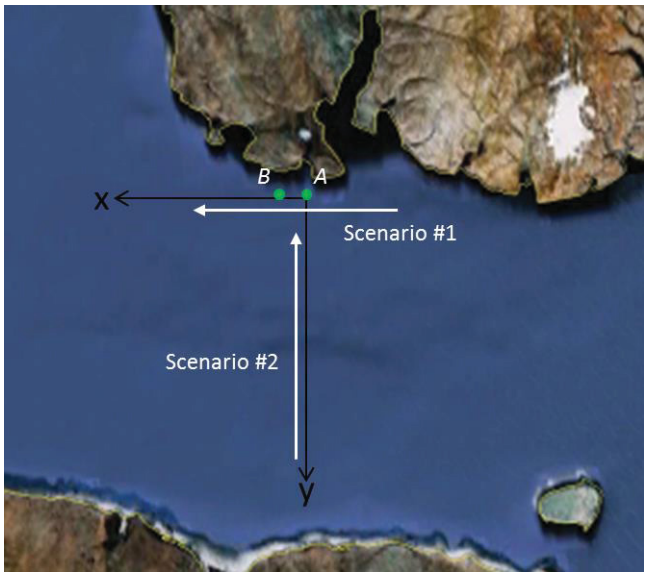

Figure 5: *Single vessel scenarios. Scenario #1 is a single vessel east-to-west transit. Scenario #2 is a single vessel south-to-north transit. Points A and B designate the locations of the acoustic arrays; the radar is assumed to be located at point A.*

All scenarios assume a low contact density, with either one or two vessels. Scenario #1 is a single vessel travelling with constant velocity, from east to west, representative of a cruise ship following the north shore of Barrow Strait. The vessel's motion is parallel to the x-axis, with, a speed of 5 m/s (equivalent to 9.7 kts), and an initial position of (-25000 m, 5000 m). In Sections 4.1 and 4.2, tests are conducted using variations of Scenario #1, with differing values of the initial position that simulate vessel transits through Barrow Strait with varying Closest Points of Approach (CPAs) to the surveillance site. Scenario #2 is single target with constant velocity, representative of a vessel crossing Barrow Strait from south to north, and approaching the surveillance site. Target motion is parallel to the y-axis, with, a speed of -5 m/s, and an initial position of (2500 m, 60000 m). Scenarios #1 and #2 are depicted in Figure 5. Scenario #3 is similar to Scenario #1, but with two vessels moving along the same path with a separation of 1000 m. Pairs of adventure sailors exhibiting this type of behaviour were observed during Arctic trials conducted in Summer 2012 [5].

All tests were implemented using Mathematica version 10.4.1.

4.1 AIS to radar association tests

In the first set of simulations, the association of radar and AIS position reports was tested using the single report association test described in Section 3.2.1. This test is based on single AIS and radar position reports, with the two reports having identical times. Tests were conducted using the single-vessel Scenarios #1 and #2. Each simulation run consisted of 100 association tests, based on 100 sets of (x, y) position reports generated at 100 s intervals over the vessel's transit through the surveillance region. At the stated speed of 5 m/s, the time interval between reports corresponds to changes in position of 500 m. Statistics were gathered based on an ensemble of 1000 runs of the same scenario. All tests were conducted at a level of significance of 0.05. At that significance level, the threshold value for the statistical distance is 5.99, and it is expected that 5% of true associations will be rejected (or conversely, 95% of true associations will be accepted).

For all simulation runs, the radar is located at the origin. Simulated radar reports are in polar form, and are produced by perturbing the target vessel's ground-truth range and bearing from the radar location with zero-mean additive Gaussian noise. The uncertainty in the radar's position reports have the following characteristics: σ_r = 200 m; σ_β = 1.0 degree; and $\sigma_{r\beta}$ = 0 (i.e. range and bearing estimates are uncorrelated). Prior to testing for association against AIS, the radar range and bearing estimates, together with associated variances, are first converted to equivalent Cartesian (x, y) values, using the transformations in Equations (9)–(11).

Simulated AIS reports are Cartesian (x, y) values relative to the radar position. AIS is assumed to be reporting with a 'high' positional accuracy, i.e., the Position Accuracy flag in the AIS Position Report is set to 1, indicating position accuracy of ≤ 10 m. Simulated AIS reports are produced by perturbing the target vessel's ground-truth position with additive Gaussian noise having standard deviations of 10 m in both x and y (and that is uncorrelated in x and y). All simulated radar and AIS reports originate from the target vessel. There are no false alarms.

The results of AIS to radar association for Scenario #1 are summarised below. Scenario #1 consists of a single vessel moving from east to west with a velocity of (5.0 m/s, 0.0 m/s), from a starting location at (-25000 m, 5000 m) to a final location at (25000 m, 5000 m). The vessel's CPA to the radar is 5000 m. Based on the ensemble of 1000 runs of the scenario, the probability of accepting the association hypothesis is calculated at each of the 100 test locations, as shown in Figure 6. These sample probabilities are in good agreement with the theoretical value of 0.95 at each location. Calculated over the complete set of 100,000 association tests from all 100 locations, the sample probability of acceptance has a mean and standard deviation of 0.951 and 0.0073, respectively. Figure 7 illustrates the statistical distance values calculated at each of the 100 test locations for a single simulation run. Of the 100 tests, six have values that exceed the threshold value of 5.99 (the threshold value being indicated by the dashed red line in Figure 7).

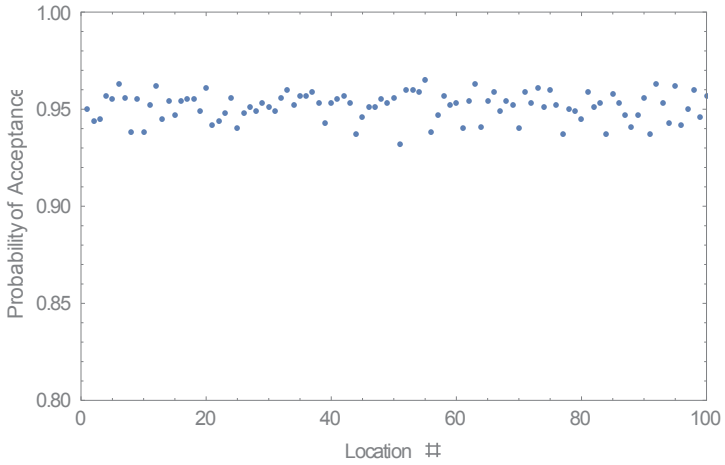

Figure 6: *Probability of accepting radar to AIS association, calculated over an ensemble of 1000 runs at each of 100 locations spaced evenly over the range (-25000 m, 5000 m) to (25000 m, 5000 m).*

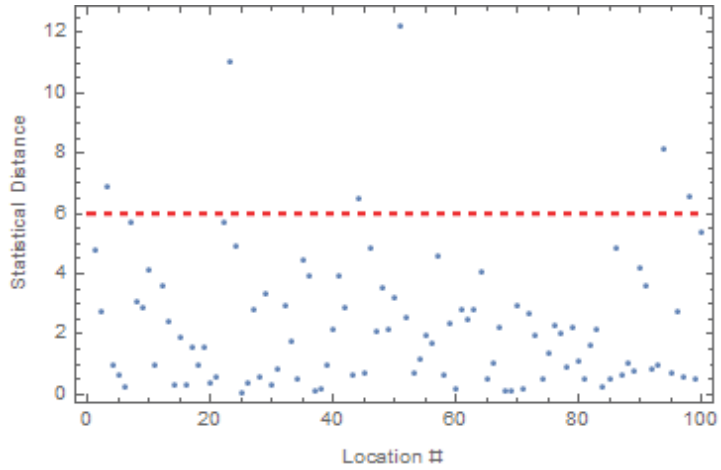

Figure 7: *Statistical distance calculated at each of 100 locations spaced evenly over the range (-25000 m, 5000 m) to (25000 m, 5000 m). The threshold value for the statistical distance, indicated by the dashed red line, is 5.99.*

The above set of tests were repeated using variations on Scenario #1, with CPA values varying between 10 km and 80 km, and using Scenario #2, which represents a south to north transit approaching the surveillance site, specified by a velocity of (0, -5.0) m/s and initial position of (0 m, 60000 m). In each case, the sample probability of accepting the association hypothesis is consistent with the significance level of the test across the entire set of test locations. This provides a strong indicator that for the given range of scenario geometries and the assumed levels of uncertainty, the non-linear transformation of radar reports from polar to Cartesian coordinates is not introducing any biases into the association tests. These test results are summarised in Table 2.

Table 2: *Probability of association hypothesis acceptance for single vessel Scenarios #1 and #2. Acceptance probabilities are calculated a set of 1000 simulation runs, with each run made up of 100 test locations. Single vessel Scenario # 1 is conducted at 6 different CPA values.*

Scenario	Velocity (m/s)	Initial position (m)	Prob. Of Accepting Association (mean ± std dev)
1	(5.0, 0.0)	(-25000, 5000)	0.951 ± 0.0073
1	(5.0, 0.0)	(-25000, 10000)	0.951 ± 0.0067
1	(5.0, 0.0)	(-25000, 20000)	0.950 ± 0.0065
1	(5.0, 0.0)	(-25000, 40000)	0.950 ± 0.0066
1	(5.0, 0.0)	(-25000, 60000)	0.950 ± 0.0068
1	(5.0, 0.0)	(-25000, 80000)	0.948 ± 0.0068
2	(0.0, -5.0)	(0, 60000)	0.949 ± 0.0078

4.2 Comparison of AIS to UWSS association tests using acoustic bearings & cross-fixes

In a second set of simulation tests, the association of UWSS acoustic bearings and AIS position reports was compared against the association of UWSS cross-fixes and AIS position reports. Given an AIS position report and UWSS acoustic bearing reports from each of the two arrays, the following two association tests are applied:

1. The combined bearing association test described in Section 3.2.6 is used to test the association of the AIS report against the two acoustic bearings.

2. A UWSS cross-fix is computed from the two acoustic bearings. The AIS position report to UWSS cross-fix report association test is then applied, using the statistical distance described in Section 3.2.2.

All hypothesis tests use the single report formulations described in Section 3.2; that is, each hypothesis test is based on a single measurement from each sensor, obtained at the same instant in time. The significance level used for all tests is 0.05.

Simulation tests were conducted using the single vessel Scenarios #1 and #2 described in Section 4.1. The acoustic centres of arrays *A* and *B* are located at (0 m, 0 m) and (5000 m, 0 m), respectively. The *x*-component of the starting location in Scenario #1 is shifted slightly, from -25000 m to -22500 m, so as to center the runs with respect to the two arrays. Similarly, the *x*-component of Scenario #2 is shifted from 0 m to 2500 m so as to center the cross-channel run between the two arrays. As with the AIS-to-radar association tests described in Section 4.1, each set of simulation tests consists of an ensemble of 1000 runs of the scenario. Individual runs consist of association tests carried out at 100 locations, with a 500 m spacing (or equivalently a 100 s interval) between test locations.

At certain vessel locations, for example long ranges, the difference between the ground truth bearings to the vessel from the two arrays may be on the same order of magnitude as the bearing uncertainty. In such a case, it is possible to generate pairs of reports whose bearings diverge rather than converge, with the result being cross-fix positions that are located behind the array. Such reports have been excluded from the analysis of association tests. Their inclusion would make the UWSS cross-fix-to-AIS association results worse than what is reported below.

Using the baseline version of Scenario #1—the east-to-west transit with a CPA of 5000 m—sample acceptance probabilities for UWSS bearing-to-AIS associations and UWSS cross-fix-to-AIS associations were computed as a function of contact location, with the results summarized in Figure 8 to 11. Consistent with the results of radar-to-AIS association tests described in the previous section, the probability of accepting the UWSS bearing-to-AIS association test is consistent with the significance level of the test and, as shown in Figure 8, this result is maintained across the set of tested locations. By comparison, the probability of accepting the UWSS cross-fix-to-AIS association tests is consistent with the test's significance level only within a restricted set of locations close to CPA,[3] as shown in Figure 9. Outside this region, the probability of acceptance decreases with distance from CPA, falling to a value of approximately 0.35 at the extremities of the run.

The test results of Scenario #1 can also be compared on the basis of the characteristics of the statistical distance. In Figure 10, the statistical distance for UWSS bearing-to-AIS association is shown as a function of test location, for a single run. Seven out of 100 tests exceed the threshold value, with the largest distance having a value of approximately 10.5. In contrast, the statistical distance for UWSS cross-fix-to-AIS associations, shown in Figure 11, exceeds the threshold at 30 out of 100 locations. These locations are predominantly at the extremities of the run, with the maximum statistical distance being 7516.

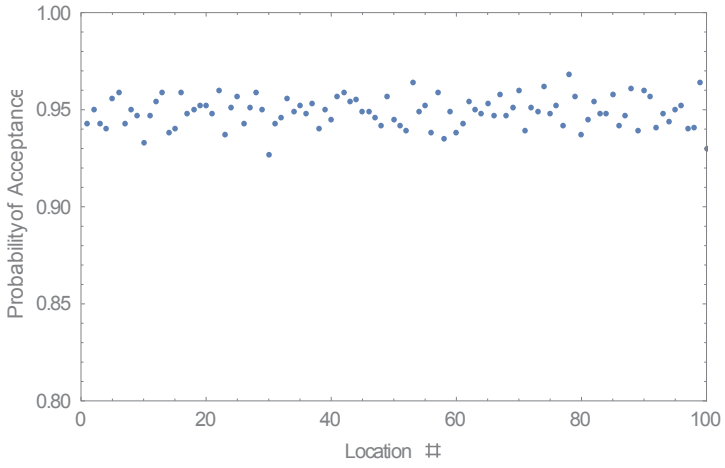

Figure 8: *Probability of accepting UWSS bearing to AIS associations, calculated over an ensemble of 1000 runs at each of 100 locations spaced evenly over the range (-22500 m, 5000 m) to (22500 m, 5000 m).*

[3] Roughly, locations 40–60, with a corresponding range of x coordinates values between -2500 to 7500 m.

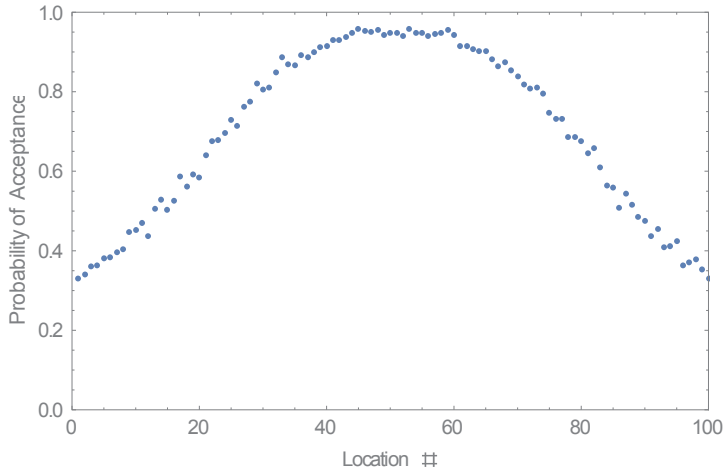

Figure 9: *Probability of accepting UWSS cross-fix-to-AIS associations, calculated over an ensemble of 1000 runs at each of 100 locations spaced evenly over the range (-22500 m, 5000 m) to (22500 m, 5000 m).*

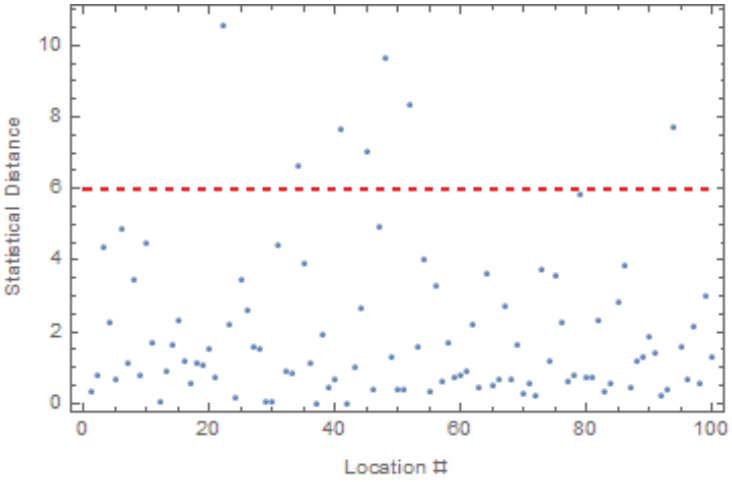

Figure 10: *Statistical distance for UWSS bearing-to-AIS associations calculated at each of 100 locations spaced evenly over the range (-22500 m, 5000 m) to (22500 m, 5000 m). The threshold value for the statistical distance, indicated by the dashed red line, is 5.99.*

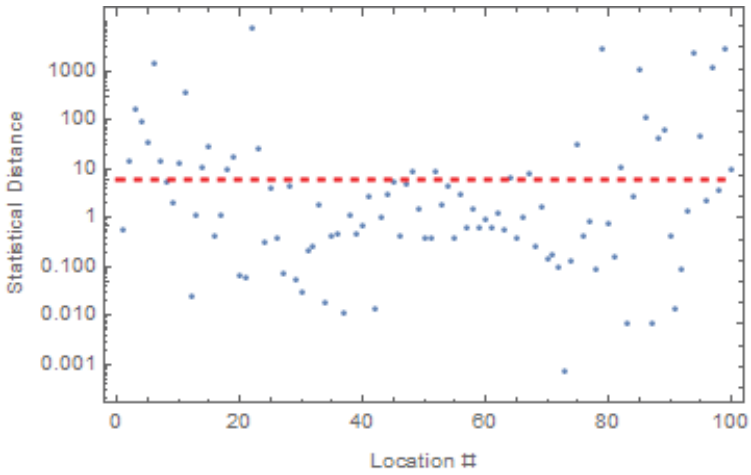

Figure 11: *Statistical distance for UWSS cross-fix-to-AIS associations calculated at each of 100 locations spaced evenly over the range (-22500 m, 5000 m) to (22500 m, 5000 m). Note that the scale used for the statistical distance is logarithmic.*

Tests using Scenario #1 were repeated at the five CPA values considered in Section 4.1: 10000 m; 20000 m; 40000 m; 60000 m; and 80000 m. The probabilities of accepting UWSS cross-fix-to-AIS associations as a function of test location are summarised in Figure 12. Two primary observations can be made. First, as CPA increases the acceptance probability is less dependent on test location (i.e. the curves become progressively flatter). Second, the maximum value of the acceptance probability, which occurs at about CPA (or equivalently, the mid-point between the arrays), is observed to decrease as CPA increases. At a CPA of 5000 m, the maximum value of the acceptance probability is 0.95 (i.e., consistent with the test's significance level); but as CPA increases to 80000 m, maximum probability is approximately 0.8. A similar relation between range and acceptance probability is observed in the results of UWSS cross-fix-to-AIS association tests for the cross-strait Scenario #2, as shown in Figure 13. At the initial location, (2500 m, 60000 m), the association probability is between 0.8 and 0.85. There is a linear increase in association probability with decreasing range, so that at the final location, (2500 m, 10000 m), the association probability is approximately 0.95.

To summarise, in using UWSS cross-fixes for association, the probability of accepting an association test is observed to be consistent with the test's significance level only for a narrow range of sensor vessel geometries that are at close ranges to both arrays. The underlying causes for these results are considered at greater length in Section 4.2.2. In contrast to the test results for UWSS cross-fix-to-AIS association, the probabilities of accepting UWSS bearing-to-AIS associations are consistent with the test significance level across all variations of Scenario #1 and for Scenario #2. This is summarized in Table 3. In all cases, the association acceptance probability is consistent across test locations, as exemplified by Figure 8.

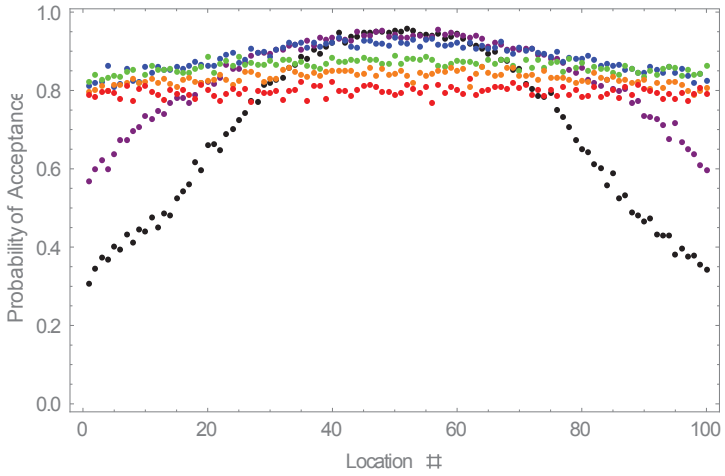

Figure 12: *Probability of accepting UWSS cross-fix to AIS associations as a function of location for variations on Scenario #1 conducted at 6 different CPA values. Scenario runs consist of the straight-line trajectories from (-22500 m, CPA) to (22500 m, CPA), where the values of CPA and corresponding run color codes (in brackets) are: 5000 m (black), 10000 m (purple), 20000 m (blue), 40000 m (green), 60000 m (orange), and 80000 m (red).*

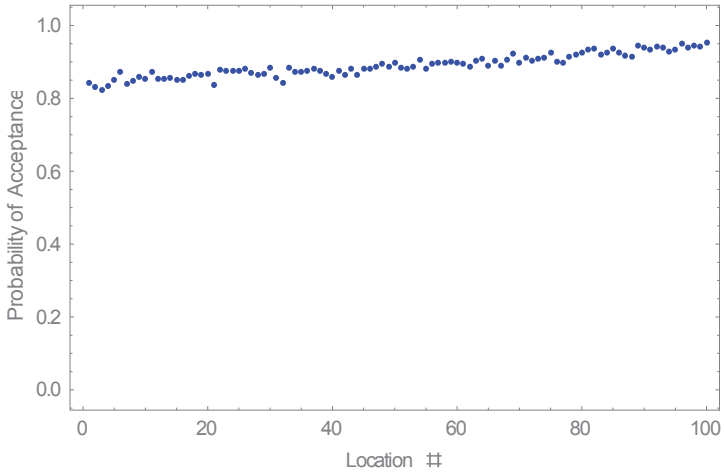

Figure 13: *Probability of accepting UWSS cross-fix to AIS associations as a function of location for the cross-strait Scenario #2. The scenario is a straight line trajectory from (2500 m, 60000 m) to (2500 m, 10000 m).*

Table 3: *Probability of accepting UWSS bearing-to-AIS association for single vessel Scenarios #1 and #2. Acceptance probabilities are calculated a set of 1000 simulation runs, with each run made up of 100 test locations.*

Scenario	Velocity (m/s)	Initial position (m)	Prob. Of Accepting Association (mean ± std dev)
1	(5.0, 0.0)	(-25000, 5000)	0.949 ± 0.0079
1	(5.0, 0.0)	(-25000, 10000)	0.950 ± 0.0076
1	(5.0, 0.0)	(-25000, 20000)	0.951 ± 0.0065
1	(5.0, 0.0)	(-25000, 40000)	0.950 ± 0.0064
1	(5.0, 0.0)	(-25000, 60000)	0.950 ± 0.0058
1	(5.0, 0.0)	(-25000, 80000)	0.950 ± 0.0071
2	(0.0, -5.0)	(0, 60000)	0.950 ± 0.0076

In Section 3.2.6, two distance measures were considered for testing the association of a pair of bearings against an AIS position report—the combined bearing association test, for which results are reported above, and the intersection of single bearing association tests. The intersection of single bearing association test was discounted because of its lower significance level relative to the significance level of a single bearing association test. This is a direct result of the fact that the intersection is rejected if either of the two individual bearing association tests is rejected. The two distance measures were compared using the baseline version of Scenario #1 and, as shown in Figure 14, the probabilities of accepting a UWSS bearing-to-AIS association are in accordance with theory. The intersection of individual bearing association has a sample acceptance probability of 0.902 ± 0.010, which is consistent with the theoretical value of 0.903, given a single bearing association test significance level of 0.05.

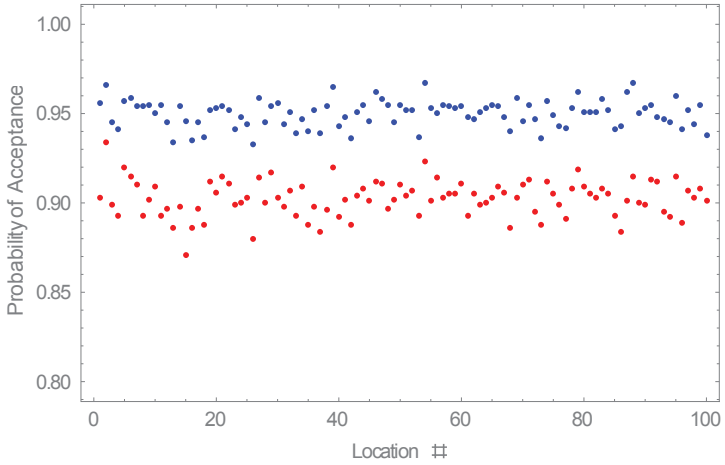

Figure 14:*.Probability of accepting UWSS bearing-to-AIS associations using the combined bearing association test (blue) and the intersection of single array tests (red).*

4.2.1 Bearing difference covariance measurements

The combined bearing association test, proposed for AIS to UWSS bearing-pair association in Section 3.2.6, makes use of the simplified expression $\hat{\delta}_A^2/\sigma_{\delta_A}^2 + \hat{\delta}_B^2/\sigma_{\delta_B}^2$ for the statistical distance in Equation (32). This simplification is based on the assumption that the covariance $\sigma_{\delta_A\delta_B}$ between bearing difference estimates $\hat{\delta}_A$ and $\hat{\delta}_B$ is negligible and can be neglected. However, given that $\hat{\delta}_A$ and $\hat{\delta}_B$ are based on a common AIS position estimate, is this assumption justified?

The assumption was tested by comparing covariance and correlation coefficient values generated using the combined bearing association against a baseline in which bearing difference estimates are computed using two independent AIS position estimates. Tests were conducted under a variety of array-to-contact geometries and bearing variances.

As in Section 3.2.6, we define the bearing difference estimates $\hat{\delta}_A = \hat{\beta}_A - \hat{\beta}_{AIS(A)}$ and $\hat{\delta}_B = \hat{\beta}_B - \hat{\beta}_{AIS(B)}$, where $\hat{\beta}_A$ and $\hat{\beta}_B$ are bearing estimates from arrays *A* and *B*, and $\hat{\beta}_{AIS(A)}$ and $\hat{\beta}_{AIS(B)}$ are the equivalent AIS bearings, relative to the locations of arrays *A* and *B*, respectively. Bearing difference estimates are generated under the following two conditions:

1. $\hat{\beta}_{AIS(A)}$ and $\hat{\beta}_{AIS(B)}$ are generated using a single AIS position estimate $\hat{\mathbf{x}}_{AIS}$ according to Equation (26). This is the condition under which the combined bearing association test is derived in Section 3.2.6.

2. $\hat{\beta}_{AIS(A)}$ and $\hat{\beta}_{AIS(B)}$ are each generated using an independent AIS position estimate.

Under each test condition the sample covariance and the sample correlation coefficient are calculated based on 1000 samples each of $\hat{\delta}_A$ and $\hat{\delta}_B$. The sample covariance $\sigma(\delta_A, \delta_B)$ is defined as

$$\sigma(\delta_A, \delta_B) = \frac{1}{n-1}\sum_{i=1}^{n}\left(\hat{\delta}_{Ai} - \bar{\delta}_A\right)\left(\hat{\delta}_{Bi} - \bar{\delta}_B\right) \tag{38}$$

where $\hat{\delta}_{Ai}$ and $\hat{\delta}_{Bi}$ are the *i*-th estimates of δ_A and δ_B, $\bar{\delta}_A$ and $\bar{\delta}_B$ are the sample means of δ_A and δ_B, respectively, and *n* is the number of samples. The sample correlation coefficient $r(\delta_A, \delta_B)$, defined as

$$r(\delta_A, \delta_B) = \frac{\sum_{i=1}^{n}(\hat{\delta}_{Ai} - \bar{\delta}_A)(\hat{\delta}_{Bi} - \bar{\delta}_B)}{\sqrt{\sum_{i=1}^{n}(\hat{\delta}_{Ai} - \bar{\delta}_A)^2}\sqrt{\sum_{i=1}^{n}(\hat{\delta}_{Bi} - \bar{\delta}_B)^2}}, \tag{39}$$

is the sample covariance normalised by the standard deviations in $\hat{\delta}_A$ and $\hat{\delta}_B$. Because the correlation coefficient is normalised to the range (-1, 1), this allows for a more straightforward comparison of results made under different test conditions.

Using 1000 samples, a substantial variation in covariance and correlation coefficient values was observed over multiple iterations using the same test conditions. In order to quantify this variation, the mean and standard deviation of the sample covariance and correlation coefficient were calculated using a set of 1000 sample values.

Test results are summarized in Table 4 and Table 5 for correlation coefficient and covariance, respectively. Test cases 1 and 2 represent vessel locations along the mid-point between the two arrays—with case #1 at a close range of 2758 m from both arrays and case two at a longer range of 28864 m from both arrays. Variances for UWSS bearing and equivalent AIS bearings are representative of the two vessel-array geometries. In each test it is observed that the mean correlation coefficients are close to zero relative to the standard deviation, regardless of whether common or independent AIS values are used. This result is attributed to the small size of the AIS bearing uncertainty relative to the UWSS bearing uncertainties. This conjecture was tested in cases 3 and 4 by reversing the uncertainties used for test cases 1 and 2, such that the UWSS bearing uncertainty was small relative to AIS. Under these conditions, a clear difference is observed between common and independent AIS measurements. In test case 4, for example, the correlation coefficient is 0.9847 when a common AIS position estimate is used versus -8.612×10^{-5} for independent AIS position estimates. The common AIS measurement clearly introduces correlation between the bearing difference estimates when the AIS bearing variance is large relative to the UWSS bearing variance.

In summary, it is concluded that so long as the equivalent bearing variance of the common AIS estimate is small relative to the UWSS bearing variances, the common AIS position estimate will not introduce significant covariance between the bearing difference estimates from the two arrays, and the simplified expression for the statistical distance in Equation (32) can therefore be applied.

Table 4: *Comparison of correlation coefficient between bearing difference estimates for common and independent AIS reports.*

Test Case	β_A (deg)	β_B (deg)	$\sigma_{\beta_{UWSS}}$ (deg)	$\sigma_{\beta_{AIS}}$ (deg)	$r(\delta_A, \delta_B)$—common AIS	$r(\delta_A, \delta_B)$—independent AIS
1	25.0	155.0	5.5	0.21	0.0008828±0.03187	0.001811±0.03187
2	85.0	95.0	2.25	0.020	0.001072±0.03093	0.0001008±0.03093
3	25.0	155.0	0.21	5.5	-0.6318±0.05097	0.0006984±0.03177
4	85.0	95.0	0.02	2.25	0.9847±0.0009758	-0.00008612±0.03094

Table 5: *Comparison of covariance between bearing difference estimates for common and independent AIS reports.*

Test Case	β_A (deg)	β_B (deg)	$\sigma_{\beta_{UWSS}}$ (deg)	$\sigma_{\beta_{AIS}}$ (deg)	$\sigma(\delta_A, \delta_B)$—common AIS	$\sigma(\delta_A, \delta_B)$—independent AIS
1	25.0	155.0	5.5	0.21	$8.474\times10^{-6}\pm0.0002937$	$1.707\times10^{-5}\pm0.0002937$
2	85.0	95.0	2.25	0.020	$1.684\times10^{-6}\pm4.771\times10^{-5}$	$1.583\pm4.771\times10^{-5}$
3	25.0	155.0	0.21	5.5	$-5.894\times10^{-3}\pm4.365\times10^{-4}$	$7.035\times10^{-6}\pm2.961\times10^{-4}$
4	85.0	95.0	0.02	2.25	$1.523\times10^{-3}\pm7.008\times10^{-5}$	$-1.639\times10^{-7}\pm4.776\times10^{-5}$

4.2.2 Limitations of first-order mean & covariance estimates for UWSS cross-fixes

In Section 4.2, it was observed that for UWSS cross-fix-to-AIS association tests, as a vessel's distance from CPA is increased, and as the bearing to the vessel approaches either 0 or 180 degrees, an increasingly large percentage of the tests are rejected relative to the tests' significance level. In other words, the tests are becoming less and less consistent with theory. One important assumption underlying the hypothesis test is that track state estimates are Gaussian distributed, with means and covariances that are consistent with stated values. In this section several examples are presented to illustrate that this assumption does not always hold in the case of UWSS cross-fixes, given the first-order approximation used to calculate the cross-fix means and covariances.

The first-order approximations for the cross-fix mean and covariance, specified in Equations (13)–(19) in Section 3.1.4, are functions of the specified means and variances of the bearing estimates from arrays A and B, and the inter-array distance. In each example presented below, the means and covariances calculated using the first-order approximations are compared against sample distributions calculated using sets of randomly generated cross-fixes. In each case 1000 cross-fix samples are generated using 1000 pairs of Gaussian-distributed bearing samples from the two arrays.

Example 1, shown in Figure 15, illustrates the cross-fixing of a contact that is on the axis equidistant between the arrays, at location (2500 m, 5000 m). This position corresponds to sample #50 in Figure 12, and falls in the region where the measured association acceptance probability is consistent with the test's significance value. In this case there is good agreement between the sample mean and the first-order mean (the red and green dots, respectively, in Figure 15) and the sample and first-order covariance (the red and green ellipses, respectively, in Figure 15). The cross-fix samples appear to be evenly distributed over the 95% quantile ellipse of the first-order covariance.

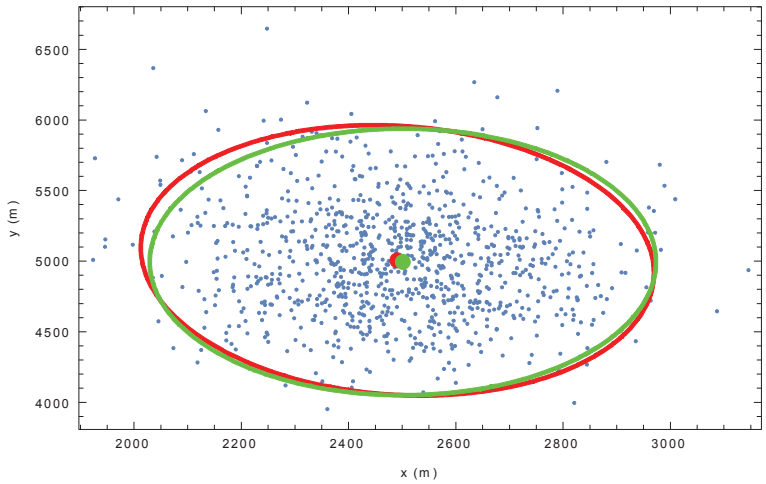

Figure 15: *Cross-fix Example 1. Sample cross-fixes (blue), sample mean and 95% quantile covariance ellipse (red) compared against first-order mean and 95% quantile covariance ellipse (green) for UWSS cross-fixes, for an object located at position (2500 m, 5000 m). β_A = 63.4 degree, β_B = 116.6 degree, and $\sigma_{\beta_A} = \sigma_{\beta_B}$ = 2.5 degree. Sample mean = {2489.8 m, 5011.3 m}. First-order mean = {2500.0 m, 5000.0 m}.*

Example 1 can be compared with the results for Examples 2–4. In Examples 2 and 3, shown in Figure 16 and Figure 17, the ground-truth locations are also located on the axis between the arrays but at progressively longer ranges, with Example 2 located at (2500 m, 20000 m) and Example 3 located at (2500 m, 40000 m). As range increases, the sample distribution becomes noticeable more fan-shaped than Gaussian, with greater numbers of sample points falling outside the 95% quantile covariance ellipse for the first-order distribution. There is a bias between the sample mean and the first-order mean and, as well, a significant increase in the size of the sample covariance relative to the first-order covariance. Similar observations can be made for cross-fixes generated in Example 4, for an off-axis vessel location, at (10000 m, 5000 m), as shown in Figure 18.

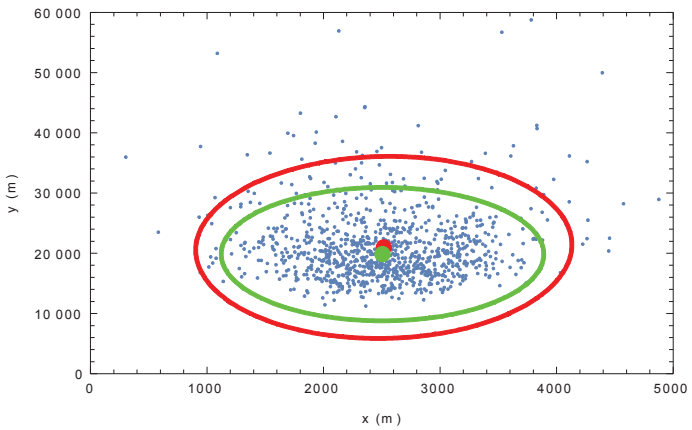

Figure 16: *Cross-fix Example 2. Sample cross-fixes (blue), sample mean and 95% quantile covariance ellipse (red) compared against first-order mean and 95% quantile covariance ellipse (green) for UWSS cross-fixes, for an object located at position (2500 m, 20000 m). β_A = 82.9 degree, β_B = 97.1 degree, and $\sigma_{\beta_A} = \sigma_{\beta_B}$ = 2.3 degree. Sample mean = {2511.2 m, 21115.6 m}. First-order mean = {2500.0 m, 20000.0 m}.*

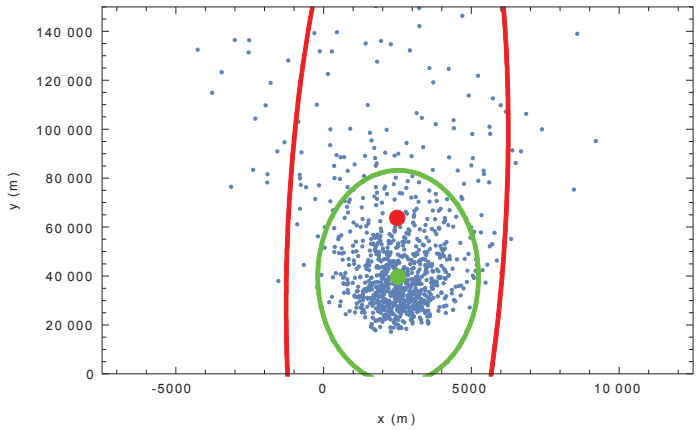

Figure 17: *Cross-fix Example 3. Sample cross-fixes (blue), sample mean and 95% quantile covariance ellipse (red) compared against first-order mean and 95% quantile covariance ellipse (green) for UWSS cross-fixes, for an object located at position {2500 m, 40000 m}.* β_A *= 86.4 degree,* β_B *= 93.6 degree, and* $\sigma_{\beta_A} = \sigma_{\beta_B}$ *= 2.3 degree. Sample mean = {2468.4 m, 64096.4 m}. First-order mean = {2500.0 m, 40000.0 m}.*

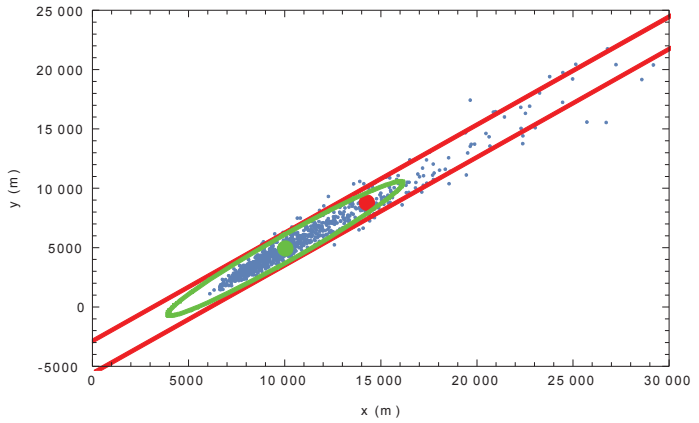

Figure 18: *Cross-fix Example 4. Sample cross-fixes (blue), sample mean and 95% quantile covariance ellipse (red) compared against first-order mean and 95% quantile covariance ellipse (green) for UWSS cross-fixes, for an object located at position {10000 m, 5000 m}.* β_A *= 26.6 degree,* β_B *= 45.0 degree,* σ_{β_A} *= 5.1 degree, and* σ_{β_B} *= 3.2 degree. Sample mean = {14242.0 m, 8860.9 m}; first-order mean = {10000.0 m, 5000.0 m}.*

The question of what conditions need apply to a function in order to obtain accurate first-order estimates of the mean and covariance has been considered by Smith and Cheeseman [21], who assert "the function must be smooth about the estimated point over an interval roughly the standard deviation of the variable." Placing this guidance in the context of acoustic cross-fixes, the x and y components of $\hat{\mathbf{x}}_{UW}$ in Equation (12) both have the term $\sin(\hat{\beta}_B - \hat{\beta}_A)$ in the denominator. As vessel range increases, $\hat{\beta}_A$ approaches $\hat{\beta}_B$ and $\hat{\mathbf{x}}_{UW}(t)$ becomes increasingly non-linear (with asymptotes occurring at $\hat{\beta}_A = \hat{\beta}_B$). The second factor that affects the accuracy of first-order estimates is the standard deviation of the bearing estimates, as a larger standard deviation imposes a wider constraint on the smoothness of the cross-fix function. Given that the standard deviation of the bearing estimates increases significantly as one approaches the angles of

0 and 180 degrees, it is expected that the accuracy of the cross-fix function also would be affected at these angles. This is consistent with simulation results in Figure 12 and Figure 13. The largest inconsistency between association test acceptance probabilities and test significance values occurred for the vessel trajectory with a CPA of 5000 m, at the extremities of the run—a set of conditions which involved both longer ranges, and hence similar bearings measurements from both arrays, and bearings that were the closest to 0 and 180 degrees.

4.3 Comparison of multiple report & single report association

In this section, the multiple report association test is demonstrated, and compared against the single report association test, for UWSS bearing and AIS tracks and a multiple vessel scenario. The scenario, designated scenario #3, is a two vessel version of scenario #1. Vessels 1 and 2 move from east to west with a velocity of (5.0 m/s, 0.0 m/s), separated by 1000 m, with vessel 1 having an initial position (-21500 m, 5000 m) and vessel 2 having an initial position of (-22500 m, 5000 m). The CPA to the arrays for both vessels is 5000 m.

Single report and multiple report association tests are conducted using AIS position reports and UWSS bearing reports from array A, located at (0,0). A sequence of 100 AIS reports and UWSS bearing reports are received for both vessels at times $\{t_k, k = 1, \dots, 100\}$, with reports occurring at 100s intervals. At each time t_k, AIS position reports $\mathbf{x}_{AIS}^1(t_k)$ and $\mathbf{x}_{AIS}^2(t_k)$ and UWSS bearing reports $\beta_{UW}^1(t_k)$ and $\beta_{UW}^2(t_k)$ are generated from vessels 1 and 2, respectively.

Single report association tests between AIS position reports and UWSS bearing reports were carried out using the procedure described in Section 3.2.4; that is, AIS position reports are first transformed into an equivalent AIS bearing and the statistical distance is calculated using the expression in Equation (30). Tests were conducted at each of the 100 times, for each of the following four combinations of AIS position report and UWSS bearing report:

- AIS position report $\mathbf{x}_{AIS}^1(t_k)$ and UWSS bearing report $\beta_{UW}^1(t_k)$, both from vessel 1, designated as $D\left(\hat{\delta}_{AIS,UW}^{1,1}(t_k)\right)$
- AIS position report $\mathbf{x}_{AIS}^1(t_k)$ from vessel 1 and UWSS bearing report $\beta_{UW}^2(t_k)$ from vessel 2, designated as $D\left(\hat{\delta}_{AIS,UW}^{1,2}(t_k)\right)$
- AIS position report $\mathbf{x}_{AIS}^2(t_k)$ from vessel 2 and UWSS bearing report $\beta_{UW}^1(t_k)$ from vessel 1, designated as $D\left(\hat{\delta}_{AIS,UW}^{2,1}(t_k)\right)$
- AIS position report $\mathbf{x}_{AIS}^2(t_k)$ and UWSS bearing report $\beta_{UW}^2(t_k)$, both from vessel 2, designated as $D\left(\hat{\delta}_{AIS,UW}^{2,2}(t_k)\right)$

All tests were conducted at a significance level of 0.05.

Single report test results are presented in Figure 19 and Figure 20. The statistical distances $D\left(\hat{\delta}_{AIS,UW}^{1,1}(t_k)\right)$ and $D\left(\hat{\delta}_{AIS,UW}^{2,1}(t_k)\right)$, between UWSS track 1 and AIS track 1 (red dots) and between UWSS track 1 and AIS track 2 (blue dots), respectively, are shown at each of the 100 times in Figure 19. The threshold distance for the hypothesis test is 3.84, as indicated by a row of green dots in the figure. Corresponding tests results for $D\left(\hat{\delta}_{AIS,UW}^{1,2}(t_k)\right)$ and $D\left(\hat{\delta}_{AIS,UW}^{2,2}(t_k)\right)$ between UWSS track 2 and each of AIS tracks 1 and 2 are shown in Figure 20. In Figure 19, the

distances $D\left(\hat{\delta}^{1,1}_{AIS,UW}(t_k)\right)$ (red dots) are true associations; in Figure 20, the true associations are the distances $D\left(\hat{\delta}^{2,2}_{AIS,UW}(t_k)\right)$ (blue dots). If one considers either of these two figures, it is observed that for a significant fraction of the updates, the hypothesis test yields ambiguous results, as both AIS contacts are accepted as possible associations with the UWSS bearing. This occurs primarily for updates 1–30 and 60–100, when both vessels have similar bearings relative to the array bearing uncertainty.

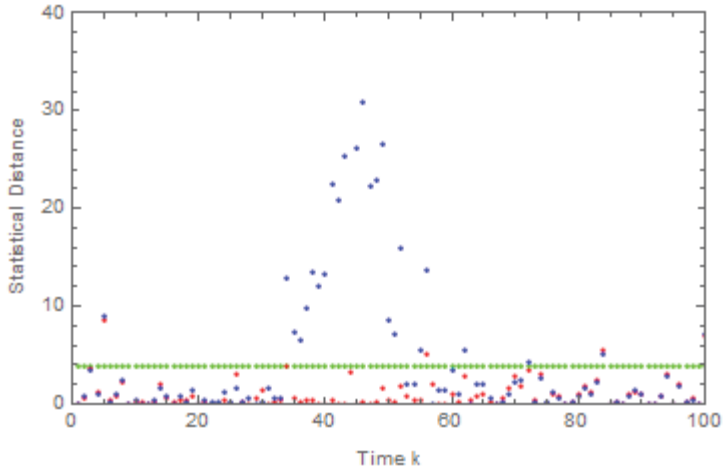

Figure 19: *Single report statistical distances, $D^{1,1}_{AIS,UW}(t_k)$ (red) and $D^{2,1}_{AIS,UW}(t_k)$ (blue) for times t_k, k = 1, …, 100. The threshold distance for the association test is shown in green.*

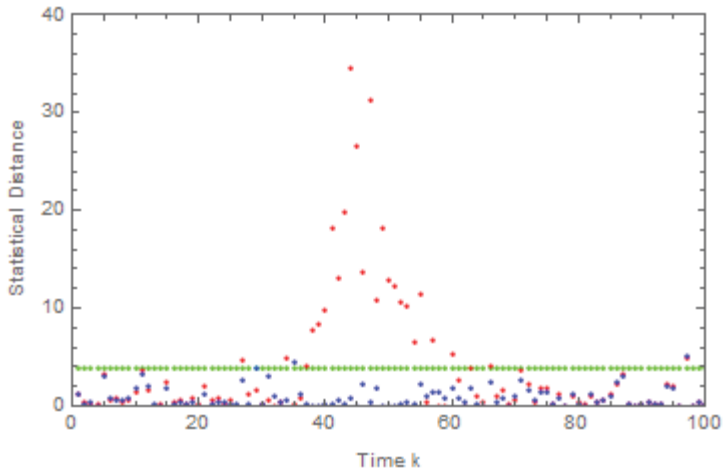

Figure 20: *Single report statistical distances, $D^{1,2}_{AIS,UW}(t_k)$ (red) and $D^{2,2}_{AIS,UW}(t_k)$ (blue) for times t_k, k = 1, …, 100. The threshold distance for the association test is shown in green.*

The multiple report association test was then applied to the single report data set described above. For each of the four combinations of AIS track and UWSS bearing track, the set $\left\{D\left(\Delta^{i,j}_{AIS,UW}(l)\right), l = 1, \ldots, 100\right\}$ of cumulative multiple-report statistical distances are calculated, where $D\left(\Delta^{i,j}_{AIS,UW}(l)\right) = \sum_{k=1}^{l} D\left(\delta^{i,j}_{AIS,UW}(t_k)\right)$ is the multiple report distance calculated over the l reports beginning at t_1 (i.e., the beginning of the scenario) and ending at time t_l.

Figure 21 shows the cumulative multi-report distances $D\left(\Delta_{AIS,UW}^{1,1}(l)\right)$ (red dots) and, $D\left(\Delta_{AIS,UW}^{1,2}(l)\right)$ (blue dots) between UWSS track 1 and each of AIS tracks 1 and 2. These are shown as a function of the number of reports used in the test. Therefore the multi-report distances at t_{100} are the result of applying the association test over the entirety of the tracks. The threshold distance, shown in green, is an increasing function of the number of reports l, in accordance with the distribution of $D\left(\Delta_{AIS,UW}^{i,j}(l)\right)$, which is approximately χ^2 with l degrees of freedom. Using the cumulative statistical distance, the correct association between AIS track 1 and UWSS bearing track 1 is maintained below the threshold over the duration of the run, independent of the number of reports used in the test. In contrast, the cumulative statistical distance for the incorrect association between UWSS bearing track 1 and AIS track 2 exceeds the threshold once approximately 30 reports are accumulated, and continues to be significantly above threshold as additional reports are taken into account, resulting in an unambiguous association decision. Similar observations can be made in regards to the cumulative multi-report distances $D\left(\Delta_{AIS,UW}^{2,1}(l)\right)$ and, $D\left(\Delta_{AIS,UW}^{2,2}(l)\right)$ between UWSS track 2 and each of AIS tracks 1 and 2, as shown in Figure 22.

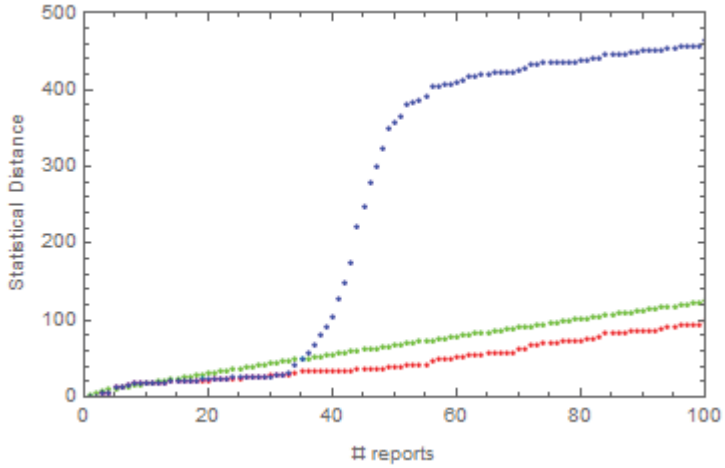

Figure 21: *Cumulative multi-report statistical distances* $D\left(\Delta_{AIS,UW}^{1,1}(l)\right)$*(red) and* $D\left(\Delta_{AIS,UW}^{2,1}(l)\right)$*(blue).*

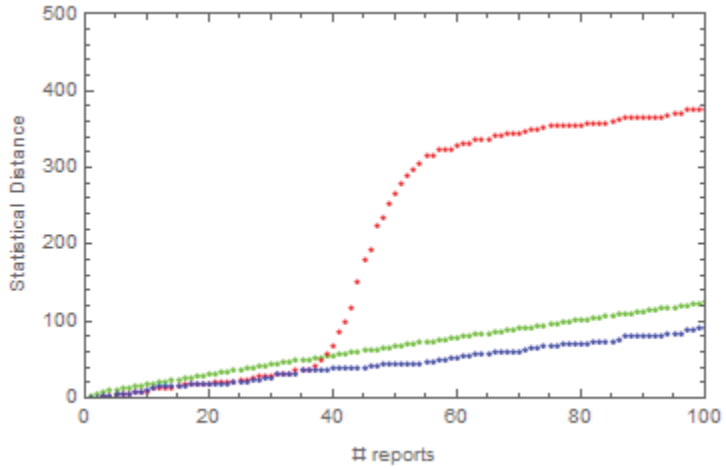

Figure 22: *Cumulative multi-report statistical distances* $D\left(\Delta^{1,2}_{AIS,UW}(l)\right)$*(red) and* $D\left(\Delta^{2,2}_{AIS,UW}(l)\right)$*(blue).*

5 Conclusions

The concept for maritime chokepoint surveillance demonstrated by DRDC's Northern Watch project relies on the integration of information from multiple above-water and underwater sensors. Achieving integrated surveillance information requires a data association process, to determine if data elements reported by different sensors correspond to the same detected platform. The manual data association capability currently implemented in the Northern Watch system has been judged to be insufficient to meet requirements of the surveillance concept. This Scientific Report documents the study of one approach to data association, based on statistical hypothesis tests, for application to the automated or semi-automated association of track data produced by the Northern Watch sensors.

The Scientific Report reviews data association requirements for an unmanned Arctic surveillance system. These derive in part from the overarching requirement to produce a complete and consistent surveillance picture. Other factors affecting data association requirements include the characteristics of sensors and vessel traffic, as well as desired modes of operator interaction using a remote controlled, unmanned system. Tracks generated by the UWSS system pose greater complexity for data association than other above-water sensor tracks for reasons that include multiple acoustic tracks generated for a single detected object, conical beam patterns, and complex three-dimensional signal propagation.

Two variants of the statistical hypothesis test are considered for use with Northern Watch sensors—a single report test based on a pair of measurements from two sensors at a single instant in time and a multiple report test based on a sequence of measurements from each sensor. Single report tests are formulated for testing the association between sensor tracks of the following types: 1D bearing estimates representative of an UWSS bearing report; 2D position estimates representative of a UWSS cross-fix report; 2D position estimates representative of information derived from an AIS position report; and 2D polar (range, bearing) position estimates representative of a radar track report. A general expression for a multiple report association test, as well a specific formulation for testing the association between UWSS bearing tracks and AIS tracks, is provided.

Consideration is given to an association test for use between an above-water sensor track and bearing tracks from each underwater array. One option is to formulate the test as the logical intersection of tests between the above-water sensor track and the bearing track on each array. An alternative option is to use a single test based on the combination of data from the above-water sensor and both arrays. The single combined test has a greater significance level relative to the intersection of single-array tests; however, this test also assumes that the cross-covariance between bearing differences, introduced by using a common AIS measurement, can be ignored. Based on simulation, this assumption was found to hold for representative sensor bearing variances.

Both single report and multiple report association tests were demonstrated using simulation. Test results were evaluated on the consistency between the percentage of rejected true associations and the level of significance of the hypothesis test. The primary findings of these tests include:

- Single report tests of the association of AIS and radar are consistent with the significance level of the test over a wide range of geometries.

- Single report tests of the association of UWSS bearings and AIS provide more consistent results when compared against tests of the association of UWSS cross-fixes and AIS. The poor performance observed using UWSS cross-fixes results from the non-linear transformation used to compute cross-fixes from bearing measurements. This transformation does not consistently preserve the Gaussian nature of the underlying bearing distributions, with the result that the sample cross-fix data may not match the modelled first-order mean and covariance estimates assumed by the hypothesis tests.
- In the case of multiple vessel scenarios with ambiguous associations, the multiple report test yields more clear and consistent results relative to the single report test.

This investigation provides a foundation for the more extensive testing of data association conducted using sensor data collected during the 2015 Final Demonstration of the Northern Watch system at Gascoyne Inlet. To conduct tests using real data sources, a number of the simplifying assumptions that were made in this study have to be taken into account. These include:

- track reports from different sensors that are not aligned in time;
- track reports that are referenced to geodetic coordinates rather than Cartesian coordinates;
- tracks that are of differing lengths; and
- the left/right ambiguity and the vertical component of UWSS conical bearings.

The results of data association tests using Arctic trials data will be published in [4].

The under-performance of association tests using UWSS cross-fixes relative to tests using UWSS bearings may have implications for information management in UWSS systems such as the DRDC Processing and Display System that was part of Northern Watch [3] . Given a situation in which a contact is detected on multiple bearing lines and on multiple arrays, it is common practice to first generate cross-fixes, and then to average multiple cross-fix position estimates. In a case where an above-water sensor is available, such as AIS or radar, it may be possible to obtain more accurate results by first associating UWSS bearings with the above-water sensor, averaging those bearings and finally generating a cross-fix position estimate.

Finally, this investigation is a source of further recommendations for the application of data association to unattended, remotely monitored, surveillance systems. In a periodic review or alerted mode of operation, a semi-automated form of picture compilation is recommended, in which: (a) the operator is responsible for maintaining the surveillance picture; and (b) for reviewing the data received since the last review/alert time. In such a situation, a cumulative, multi-report association test may be applied. All data received since the last review or alert time would be processed in batch form and a single set of association recommendations for each track provided to the operator. In a real-time mode of operation, a cumulative association test, using a short time window is recommended (with choice of time window selected to trade-off latency against association accuracy). In either mode of operation UWSS bearing data rather than UWSS cross-fix data should be used for testing for association with tracks from above-water sensors.

Using a semi-automated mode of operation, the operator should be provided with a mechanism to inspect association recommendations. This is particularly important for cases of ambiguous associations. One possibility would be to use the time histories of the association scores, similar

to the graphs shown in Section 4. Here it may be beneficial to provide the test statistic, relative to thresholds, both on a cumulative and on a report by report basis.

References

[1] McArthur, B.A., "Northern Watch System Concept V2.0," Defence R&D Canada – Atlantic, DRDC Atlantic TM 2012-119, July 2012.

[2] McArthur, B.A., "A system concept for persistent, unmanned, local-area Arctic surveillance," in Carapezzo, E.M., Datskos, P.G., Tsamis, C., Laycock, L., and White, H.J. (Eds.), *Unmanned/Unattended Sensors and SensorNetworks XI and Advanced Free-Space Optical Communication Techniques and Applications*, Proc. SPIE, vol. 9647, 2015.

[3] Heard, G.J., McArthur, B.A., and Inglis, G., "Overview of the technical results of the Northern Watch Project," Defence Research and Development Canada, DRDC Scientific Report DRDC-RDDC-2016-R115, 2016.

[4] McArthur, B.A. "Experimental tests of track association algorithms for Northern Watch," Defence Research and Development Canada, in press.

[5] McArthur, B.A., Pelavas, N., Heard, G.J., Cross, R., Brookes, D., Roy, S., and Forand, L., Private Communication.

[6] McIntyre, C.M. and Roger, W.A., "Data Association in Passive Acoustic Tracking," in Drummond, O.E. (Ed.), *Signal and Data Processing of Small Targets 1993*, Proc. SPIE, vol. 1954, pp. 376–385, 1993.

[7] Olmstead, J. "Operator Manual for Northern Watch Technology Demonstration Project," DRDC Contractor Report DRDC-RDDC-2016-C235, MDA Systems Ltd, 2016.

[8] Bar-Shalom, Y. and Fortmann, T.E., "Tracking and Data Association," Orlando, FL: Academic Press, 1988.

[9] Blackman, S. and Popoli, R., "Design and Analysis of Modern Tracking Systems," Norwood, MA: Artech House, 1999.

[10] Singer, R.A. and Kanyuck, A.J., "Computer Control of Multiple Site Correlation," Automatica, vol. 7, no. 4, pp. 455–463, 1971.

[11] Walpole, R.E. and Myers, R.H., "Probability and Statistics for Engineers and Scientists," Second edition. New York, NY: Macmillan, 1978.

[12] Garcia, J., Guerrero, J.L., Luis, A., and Molina, J.M., "Robust Sensor Fusion in Real Maritime Scenarios," Proc. Fusion 2010, paper we.1.6.3-0231.

[13] Carthel, C., Coraluppi, S., and Grignan, P. "Multisensor Tracking and Fusion for Maritime Surveillance," Proc. Fusion 2007, paper Fusion2007_1224, 2007.

[14] Bick, E.T. and Barock, R.T., "CENTURIAN harbor surveillance testbed," Proc. IEEE Oceans 2005, pp. 1358–1363, 2005.

[15] Shijun, Y., Jinbiao, C., and Chaojian, S., "A Data Fusion Algorithm for Marine Radar Tracking," Proc. IEEE Global Congress on Intelligent Systems, pp. 234–238, 2009.

[16] Battistello, G., Gonzalez, J., Ulmke, M., Koch, W., Mohrdieck, C., "Multi-Sensor Maritime Monitoring for the Canadian Arctic: Case Studies," Proc. 19th Intl Conf. on Information Fusion, 2016.

[17] Trunk, G. and Wilson, J.D., "Association of DF Bearing Measurements with Radar Tracks," IEEE Trans. on Aerospace and Electronic Systems, vol. AES-23, no. 4, pp. 438–447, July 1987.

[18] La Scala, B. and Farina, A., "Effects of Cross-Correlation and Resolution on Track Association," Proc. Fusion 2000, paper WeD1-2, 2000.

[19] Gendron, J., "Evaluation of Data Associations for Active and Passive Sensors," Master's Thesis, Department of Electrical Engineering, Royal Military College, Kingston, 2001.

[20] Bar-Shalom, Y., "On the Track-To-Track Correlation Problem," IEEE Trans. Automatic Control, vol. AC-26, pp. 571–572, April 1981.

[21] Smith, R. and Cheeseman, P., "On the Representation and Estimation of Spatial Uncertainty," International Journal of Robotics Research, vol. 5, no. 4, pp. 56–68, 1986.

[22] Jazwinski, A., "Stochastic Processes and Filtering," New York, NY: Academic Press, 1970.

[23] United States Coast Guard Navigation Center, "Class A AIS Position Report (Messages 1, 2, and 3)," 2016, http://www.navcen.uscg.gov/?pageName=AISMessagesA (Access date: 29 Sept 2016).

[24] United States Coast Guard Navigation Center, "AIS Standard Class B Equipment Position Report (Message 18)," 2016, http://www.navcen.uscg.gov/?pageName=AISMessagesB (Access date: 29 Sept 2016).

[25] Urick, R., "Principles of Underwater Sound," Third edition. McGraw Hill, 1983.

[26] Heard, G.J. and Pelavas, N., "Northern Watch Underwater Sensor System Operating Concept," Defence R&D Canada – Atlantic, DRDC Atlantic TM 2011-087, 2011.

[27] Bar-Shalom, Y., "On the Sequential Track Correlation Algorithm in a Multisensor Data Fusion System," IEEE Trans. on Aerospace and Electronic Systems, vol. 44, no. 1, p. 396, January 2008.

[28] La Scala, B. and Farina, A., "Choosing a track association method," Information Fusion, vol. 3, pp. 119–133, 2002.

[29] Blackman, S., "Multiple-Target Tracking with Radar Applications," Norwood, MA: Artech House, Chapter 7, 1986.

List of symbols/abbreviations/acronyms/initialisms

ADS-B	Automatic Dependent Surveillance – Broadcast
AIS	Automatic Identification System
ASDS	Arctic Surveillance Demonstration System
COP	Common Operating Picture
CPA	Closest Point of Approach
DND	Department of National Defence
DRDC	Defence Research and Development Canada
DSCC	DRDC Southern Control Centre
ICAO	International Civil Aviation Organization
IMO	International Maritime Organization
MMSI	Maritime Mobile Service Identity
NTP	Network Time Protocol
UWSS	Underwater Sensor System

This page intentionally left blank.

DOCUMENT CONTROL DATA

(Security markings for the title, abstract and indexing annotation must be entered when the document is Classified or Designated)

1. ORIGINATOR (The name and address of the organization preparing the document. Organizations for whom the document was prepared, e.g., Centre sponsoring a contractor's report, or tasking agency, are entered in Section 8.)

DRDC – Atlantic Research Centre
Defence Research and Development Canada
9 Grove Street
P.O. Box 1012
Dartmouth, Nova Scotia B2Y 3Z7
Canada

2a. SECURITY MARKING (Overall security marking of the document including special supplemental markings if applicable.)

UNCLASSIFIED

2b. CONTROLLED GOODS

(NON-CONTROLLED GOODS)
DMC A
REVIEW: GCEC DECEMBER 2013

3. TITLE (The complete document title as indicated on the title page. Its classification should be indicated by the appropriate abbreviation (S, C or U) in parentheses after the title.)

An investigation of track association algorithms for Northern Watch

4. AUTHORS (last name, followed by initials – ranks, titles, etc., not to be used)

McArthur, B.

5. DATE OF PUBLICATION (Month and year of publication of document.)	6a. NO. OF PAGES (Total containing information, including Annexes, Appendices, etc.)	6b. NO. OF REFS (Total cited in document.)
May 2017	56	29

7. DESCRIPTIVE NOTES (The category of the document, e.g., technical report, technical note or memorandum. If appropriate, enter the type of report, e.g., interim, progress, summary, annual or final. Give the inclusive dates when a specific reporting period is covered.)

Scientific Report

8. SPONSORING ACTIVITY (The name of the department project office or laboratory sponsoring the research and development – include address.)

DRDC – Atlantic Research Centre
Defence Research and Development Canada
9 Grove Street
P.O. Box 1012
Dartmouth, Nova Scotia B2Y 3Z7
Canada

9a. PROJECT OR GRANT NO. (If appropriate, the applicable research and development project or grant number under which the document was written. Please specify whether project or grant.)	9b. CONTRACT NO. (If appropriate, the applicable number under which the document was written.)
06ab	

10a. ORIGINATOR'S DOCUMENT NUMBER (The official document number by which the document is identified by the originating activity. This number must be unique to this document.)	10b. OTHER DOCUMENT NO(s). (Any other numbers which may be assigned this document either by the originator or by the sponsor.)
DRDC-RDDC-2017-R062	

11. DOCUMENT AVAILABILITY (Any limitations on further dissemination of the document, other than those imposed by security classification.)

Unlimited

12. DOCUMENT ANNOUNCEMENT (Any limitation to the bibliographic announcement of this document. This will normally correspond to the Document Availability (11). However, where further distribution (beyond the audience specified in (11) is possible, a wider announcement audience may be selected.))

Unlimited

13. ABSTRACT (A brief and factual summary of the document. It may also appear elsewhere in the body of the document itself. It is highly desirable that the abstract of classified documents be unclassified. Each paragraph of the abstract shall begin with an indication of the security classification of the information in the paragraph (unless the document itself is unclassified) represented as (S), (C), (R), or (U). It is not necessary to include here abstracts in both official languages unless the text is bilingual.)

The concept for Arctic maritime chokepoint surveillance demonstrated by Defence Research and Development Canada's (DRDC) Northern Watch project requires a process for data association—the determination that multiple data elements reported by different sensors correspond to the same detected platform—to enable the integration of information from multiple above-water and underwater sensors.

In response to documented shortfalls in the manual data association capability implemented in the Northern Watch system, this Scientific Report reviews the requirements for data association in the context of unmanned, remotely operated surveillance, and describes an investigation of one class of algorithm, based on statistical hypothesis tests, for application to the automated or semi-automated association of track data produced by the Northern Watch sensors. Two variants of the statistical hypothesis test are described—a single report test based on a pair of measurements from two sensors at a single instant in time and a multiple report test based on a sequence of measurements from each sensor. Test results are presented, using simulated data, for the association of bearings-only and positional cross-fix tracks from underwater acoustic arrays against AIS and radar tracks. It was found that association using underwater array bearings provides more consistent results when compared against similar tests involving the association of underwater array cross-fixes.

Le concept de surveillance des points de passage maritime obligé dans l'Arctique fournit la preuve que le projet de surveillance du Nord de Recherche et développement pour la défense Canada (RDDC) requiert un procédé d'association de données par lequel on peut établir que de multiples éléments des données recueillies par différents capteurs correspondent à une même plateforme détectée, et ce, afin de permettre l'intégration de l'information provenant de multiples capteurs en surface et sous l'eau.

En réponse aux lacunes relevées dans la capacité manuelle d'association de données mise en œuvre dans le système de surveillance du Nord, le présent rapport scientifique aborde les exigences à cet égard dans le cadre d'une télésurveillance sans opérateur et décrit l'étude d'une catégorie d'algorithmes à partir de tests d'hypothèses statistiques en vue de l'appliquer à l'association automatisée ou semi-automatisée de données de poursuite générées par les capteurs du système. Deux variantes des tests d'hypothèses statistiques sont décrites ici, soit un premier compte rendu de test unique, fondé sur les mesures provenant de deux capteurs à un instant donné, et un second compte rendu de tests multiples, fondé sur une séquence de mesures prises par chacun des capteurs. On utilise des données simulées pour comparer les résultats de tests sur l'association de pistes en mode gisement seul connu et de points par relèvements de la position à partir des réseaux acoustiques sous-marins aux pistes recueillies par sonar actif d'identification et par radar. On a découvert que l'association par mode gisement des réseaux sous-marins permettait d'obtenir des résultats plus cohérents en comparaison de ceux des points par relèvements des réseaux sous-marins.

14. KEYWORDS, DESCRIPTORS or IDENTIFIERS (Technically meaningful terms or short phrases that characterize a document and could be helpful in cataloguing the document. They should be selected so that no security classification is required. Identifiers, such as equipment model designation, trade name, military project code name, geographic location may also be included. If possible keywords should be selected from a published thesaurus, e.g., Thesaurus of Engineering and Scientific Terms (TEST) and that thesaurus identified. If it is not possible to select indexing terms which are Unclassified, the classification of each should be indicated as with the title.)

Arctic surveillance; data association; simulation